Response to referee comments on the manuscript "Observing Entrainment Mixing, Photochemical Ozone Production, and Regional Methane Emissions by Aircraft Using a Simple Mixed-Layer Model," Trousdell et al., ACP (2016)

Thanks to all the referees for their time and critiques, we benefitted greatly. All responses are in blue type with the referee comments in black.

Referee #1

The paper by Trousdell describes new aircraft measurements, which, combined with the mixed layer budget equation, attempts to constrain entrainment, advection, and the emission/production of ozone, methane and water. The dataset and analysis could be suitable for ACP, but as it stands the paper tries to address too many disparate issues: entrainment, the ozone budget, the methane budget, surface heat fluxes and the water cycle. In my opinion the paper needs to be significantly modified before publication.

As a consequence the findings are often not discussed in depth and put into context of uncertainties.

I understand how you could see that we attempt to take on disparate issues, but our goal is precisely that: to bridge dynamics and chemistry. We feel that the atmospheric chemistry and boundary layer communities can benefit from each other, and the use of this simple mixed layer model demonstrates that. This journal attracts those interested in atmospheric dynamics as well as chemistry so we believe it is the perfect fit for our manuscript. To clarify, our intention when detailing these various topics like the ozone budget, the methane budget, entrainment, etc. is not to necessarily go into great depths on each but to show how a simple mixed layer budget equation sufficiently closed by in-situ flight data, including a detailed calculation of entrainment, can be used to uncover useful and novel estimates of emissions and photochemical rates. With this in mind, and in light of the complex mesoscale environment, we feel it is inadvisable to to add all of the details from these various topics, yet it is important to present them together. The crux of this study is really the computation of dynamic quantities, like entrainment and linking them to the chemistry of the boundary layer.

On the other hand, we can see how our treatment of the uncertainties of these estimates could come across as lacking depth, so we have rewritten that entire section (4 Error Analysis) to clarify our estimates of the uncertainty of this approach.

A major uncertainty, that needs more evaluation, is the fusion of in-situ observations with large scale reanalysis data. What are the uncertainties of this approach? E.g. when extracting mean vertical wind speed or surface fluxes from

NARR, and plugging these data into eqs. (4),(6), etc., to extract small residuals of the observed quantities.

To be clear, we do not put surface fluxes nor mean vertical velocities into equations 4 and 6. The only reanalysis data we incorporate is into equation 2, the inversion height budget equation. To answer the question directly, I would refer the reviewer to Table 1, wherein it appears that the very conservative uncertainty we assign to the mean vertical velocity of the NARR (0.5 cm/s or approximately 50%) leads to large uncertainties in the derived entrainment velocities: ~1.0 cm/s for each project average (1.5 and 3.0 cm/s averages). We feel this is a reasonable estimate of this uncertainty and do propagate it through the entrainment terms in the other budget equations (4 & 6) where that term is not always the leading one, however the large uncertainties in methane emissions are a direct result of these assumed uncertainties. Therefore, we disagree with the reviewer in that this is **not** a case of trying to tease out a small residual from large terms with large uncertainties.

With regards to the suitability of our estimated uncertainty in the NARR vertical velocities, we refer to a study by Albrecht et al. (2016). They also utilized reanalysis data in the form of omega, which was later transformed to vertical velocity and subsequently used in the exact same inversion height budget equation we use. They estimated the error of the average vertical velocity derived in this fashion to be ± 0.1 cm s^{-1}, a full factor of five times smaller than ours. In addition, they conclude that the majority of variation from this budget equation is reflected in the local time rate of change of inversion height when compared to the variations in the advection of inversion height and vertical velocity combined. We also found the budget equation of inversion height to be dominated by time rate of change on average, so feel that we are measuring the most important term in the z_i governing equation (2). We have added these details to our error analysis section to help clarify these points.

Generally the paper lacks a consistent analysis of error propagation, which makes it hard to follow the uncertainty of the complex method of extracting tracer budgets.

We have expanded our error analysis section (Section 4) to include a more detailed analysis. Some of the errors were calculated formally using a standard error which is a residual from the linear fit normalized by the number of data points, but other error terms are not subject to such statistical formalism. For instance, the error in the scalar jump, which is diagnosed by eye from vertical profiles is given what we deem a conservative estimate of its error. We also note that our estimated error for vertical velocity obtained from NARR is five times greater than that used by the Albrecht et al 2016 study for the reanalysis data they used (ECMWF). We try to be careful and we include errors with every term in the budgets. For cases when terms were not subject to a rigorous mathematical analysis of error we attempt to be conservative and overestimate the potential error. In Tables 1-3 we have now included the standard deviations of the mean values from each campaign to give a

sense of the natural, background variation relative to the observational uncertainty estimates to help place these in context.

Section 3.2.1: The ozone budget has to be corrected and time-shifted due to rapid photochemistry. Is this done arbitrarily to minimize residuals?

Our ozone budgets were not time shifted or corrected for rapid photochemistry. The only instance in the manuscript where we corrected the ozone levels was to make plots of horizontal gradients and advection, which were corrected by way of the secular linear time rate of change to a common time stamp. This reduces the spatial 'noise' of the aircraft measurements which are sweeping over the region throughout the day when the mean ozone is on the rise.

Ozone production: methane is used as a VOC tracer to demonstrate that P(O3) is NOx-limited. Yet methane is not a very good tracer, because it has quite different sources compared to VOCs emitted from transport and combustion processes (e.g. aromatics). In addition biogenic VOCs are not considered at all by this approach. Methane is a fugitive emission and therefore does not represent the variation of VOC reactivity properly. To make a more convincing point the authors should use data from the parallel SEACRS mission or ground based observations in combination with a photochemical model to show what fraction of OH reactivity is due to methane (likely very small) and whether methane significantly co-varies with the local VOC reactivity.

As discussed in Section 3.2.2 the majority of methane in both studies are believed to be associated with fossil fuel extraction and dairy operations. The studies of Gentner et al. [2014] and Pusede et al. [2014] indicate that methane is fairly well correlated with alcohols (which have strong dairy sources), higher alkanes (natural gas), and CO (other anthropogenic activities.) While we acknowledge that methane is a somewhat crude tracer of reactive VOC, we present the results because there is a suggestive relationship with our inferred ozone production rates that is consistent with past studies of the ozone production regime.

With respect to the SEAC4RS dataset we found only one boundary layer leg within the Central Valley of California during that mission. With that we have about one hour of data taken in the early evening containing 28 data points from the dataset of Don Blake showing a correlation of 0.6 or greater with CH4 for; CO, DMS, HCFC-124, HFC-134a, HFC-152a, CH3I, CH2Cl2, C2HCl3, C2Cl4, MeONO2, EtONO2, i-PrONO2, n-PrONO2, 2-BuONO2, 3-Methyl-2-BuONO2, 3-PenONO2, 2-PeONO2, Ethane, Ethene, Ethyne, Propane, Propene, n-Butane, 1-Butene, i-Butene, i-Pentane, n-Pentane, 1-Pentene, 2_3-Dimethylbutane, 2-Methylpentane, 3-Methylpentane, n-Heptane, Benzene, Ethylbenzene, and beta-Pinene. From this mix of hydrocarbons we maintain that CH4 is a decent, although imperfect, tracer for other reactive hydrocarbons. Trying to use this limited data set in a photochemical model seems well beyond the scope of this paper, and the NOx-limited nature of the ozone environment has been confirmed in other studies (Pusede et al. [2012], Brune et al.,

[2016]).

In the following section (3.2.2) methane emissions are discussed, but given the uncertainty of the local methane budget (e.g. 100 +/-100Gg/yr), one wonders about the significance of the results. Again, without proper error propagation it makes it hard to follow the validity of the approach, especially uncertainties originating from the model- data fusion. The reader is left with the impression that the approach relies on luck and a fair wind.

It is true our methane emission errors are of a similar order of magnitude as the overall flight-to-flight spread. This is caused by the fact that we estimate our errors in entrainment to be nearly the same order of magnitude as the results. But this magnitude of uncertainty in entrainment is common for measurements of such a difficult, yet important, parameter (de Arellano et al. [2004] de Roode & Duynkerke, [1997]; Bretherton et al, [1995]; Wolfe et al., 2015). So, naturally emission estimates that are derived directly from this parameter are going to have similarly large uncertainties. But we believe that it is still a valid measurement, and when repeated over many flights, the mean measurement is indeed meaningful. Furthermore, this is a very important result to the methane community, which is faced with a paucity of such estimates. It also might be useful to note here that inverse modeling techniques used to derive a posteriori emission estimates likely have similarly large uncertainties, but these are rarely, if ever, explicitly treated in modeling papers (Cui et al. 2015).

Section 3.2.3: Surface latent heat flux: In my opinion this part of the paper presents the most interesting aspects, as it shows a significant bias of surface fluxes obtained from re-analysis data. Why do the authors not present a more in-depth analysis of this finding?

The calculation of the water budget was an easy addition for us because our payload measures water vapor, and since the budget equation for water does not have any internal source terms under our flight conditions. The results are included to show the robustness and wide applicability of the budget method. We agree the findings are interesting, but we leave them as general warnings to the community about the latent heat calculated in NARR, and that this is certainly going to have an effect on ABL heights due to partitioning of latent vs. sensible heat fluxes. But to probe this result more deeply would require a lot more information about the land-surface and we feel would distract from the main objective of the manuscript.

Section 4: Rather arbitrarily 5 lines of error analysis are presented here, but only address a very small part that would be necessary for the entire paper.

We agree with you that our error analysis was overly concise, and we hope that the expanded error analysis section will assuage many of your concerns.

Generally, in my opinion the paper tries to address too many disparate issues and therefore lacks in depth analysis of the individual pieces. For a focus on ozone, the authors should definitely combine their results with a more comprehensive set of chemistry observations, which seem to be available.

We believe that estimating net O3 production is a significant feat, and we have done so with equal or better uncertainty than other reports of in the literature (Pusede et al, 2014; Brune et al., 2016). Furthermore, without a vast array of chemical species and meteorological data to constrain a model, we do not feel that all that much would be gained in such an exercise.

For a focus on entrainment and PBL dynamics, a PBL model should be used in conjunction with the budget equation. The paper would also greatly benefit from a more thorough discussion of the associated uncertainties when closing the PBL budget. Perhaps a useful resource to better constrain the thermodynamical and dynamical properties of the PBL during the research flights, and address the propagation of errors and uncertainties, can be found here: http://classmodel.github.io/

We hope that in light of our responses here and above the reviewer will reconsider their conclusion that the absence of applying more complicated models to this data set is a sign of a superficial treatment of the subject. Our intention here is to present an empirical study of surface emissions, ozone photochemistry, and entrainment in the San Joaquin Valley, and the wide applicability of the airborne budget method we have applied. Perhaps our use of the term 'model' in the title is a bit misleading, because by 'model' we really mean a simple analytical tool that can be applied to airborne data. We do not wish to resort to any higher order models in this analysis, because such models necessarily require boundary conditions and initial conditions that were not constrained by observation – specifically, OH reactivity and/or speciated VOC data in the ozone analysis, and surface heat fluxes in the entrainment analysis.

We do not believe that the particular model referred to above will help us better understand uncertainty, but will rather add more. The Dutch slab model is based on many inputs including, but not limited to, surface heat fluxes, drag coefficients, initial boundary layer height, free tropospheric stability, and of course subsidence.. Additionally, the model does not include advection so we would still need some way to account for the uncertainties of this term and the subsidence term, but would have no way to know the uncertainties in the surface heat or momentum fluxes. We feel the method presented here is more direct because it is not driven by all of these unknown parameters and more closely tracks the uncertainties in the governing equations themselves, as we hope is now more clearly presented in the new section 4.

References:

Albrecht, B., Fang, M., Ghate, V.: Exploring Stratocumulus Cloud-Top Entrainment Processes and Parameterizations by Using Doppler Cloud Radar Observations, J. Atmos. Sci. 73(2), 729-42, 2016.

Bretherton, C. S., and Pincus, R.: CLOUDINESS AND MARINE BOUNDARY-LAYER DYNAMICS IN THE ASTEX LAGRANGIAN EXPERIMENTS .1. SYNOPTIC SETTING AND VERTICAL STRUCTURE, J. Atmos. Sci., 52, 2707-2723, 10.1175/1520-0469(1995)052<2707:cambld>2.0.co;2, 1995.

Cui, Y. Y., Brioude, J., McKeen, S. A., Angevine, W. M., Kim, S. W., Frost, G. J., Ahmadov, R., Peischl, J., Bousserez, N., Liu, Z., Ryerson, T. B., Wofsy, S. C., Santoni, G. W., Kort, E. A., Fischer, M. L., and Trainer, M.: Top-down estimate of methane emissions in California using a mesoscale inverse modeling technique: The South Coast Air Basin, J. Geophys. Res.-Atmos., 120, 6698-6711, 10.1002/2014jd023002, 2015.

deArellano, Vilà-Guerau, J., Gioli, B., Miglietta, F., Jonker, H. J. J., Baltink, H. K., Hutjes, R. W. A. and Holtslag, A. A. M.: Entrainment Process of Carbon Dioxide in the Atmospheric Boundary Layer, J. Geophys. Res. 109(D18), 2004.
Elsgaard, L., Olsen, A. B., and Petersen, S. O.: Temperature response of methane production in liquid manures and co-digestates, Sci Total Environ, 539, 78-84, 10.1016/j.scitotenv.2015.07.145, 2016.

deRoode, S. R., and Duynkerke, P. G.: Observed Lagrangian transition of stratocumulus into cumulus during ASTEX: Mean state and turbulence structure, J. Atmos. Sci., 54, 2157-2173, 10.1175/1520-0469(1997)054<2157:oltosi>2.0.co;2, 1997.

Gentner, D. R., Ford, T. B., Guha, A., Boulanger, K., Brioude, J., Angevine, W. M., de Gouw, J. A., Warneke, C., Gilman, J. B., Ryerson, T. B., Peischl, J., Meinardi, S., Blake, D. R., Atlas, E., Lonneman, W. A., Kleindienst, T. E., Beaver, M. R., St Clair, J. M., Wennberg, P. O., VandenBoer, T. C., Markovic, M. Z., Murphy, J. G., Harley, R. A., and Goldstein, A. H.: Emissions of organic carbon and methane from petroleum and dairy operations in California's San Joaquin Valley, Atmospheric Chemistry and Physics, 14, 4955-4978, 10.5194/acp-14-4955-2014, 2014.

Referee #2

Summary

This paper presents results from two small flight campaigns in California. Observed trace gas concentrations and profiles are used to derive entrainment velocities and examine the boundary-layer budgets of ozone, methane and water vapor. Results are used to evaluate photochemical ozone production, regional methane emissions and evapotranspiration.

The presented data is new, and the analysis of boundary layer budgets is a useful technique that is perhaps under-utilized in our field. The paper is generally well-written, although the embellished language is distracting at times and some sections provide an over-abundance of contextual details. Revisions are necessary before publication.

General Comments

Section 2.1 provides a wealth of interesting but non-essential details on the topography and meteorology of the SJV. The first three paragraphs could probably be condensed down to one by removing such details –particularly those regarding specific orographic effects, which get confusing unless one constantly refers to a map or is familiar with the area. Indeed, the third paragraph (page 4, line 13) seems totally irrelevant given that the data presented is all daytime. The last paragraph in this section reads like a primer on mountain-valley flows and again seems only tangentially relevant to the results presented later.

We understand the referee's point here, and we have condensed much of the information originally presented. We chose to include a clear survey of mountain-valley dynamics to set the stage for this unique mesoscale environment in which we are working and because we do not find such a concise treatment in the extant literature. It is exactly this dynamically complex environment which has exacerbated the markedly poor air quality in the region. For others working on the recalcitrant air quality issues in this area, or similar ones such as the Po Valley in Italy, we feel this information is essential for consideration.

The conclusions section is just a summary of main findings. It would be useful to add some discussion of needs for future work, in particular how some of the findings (such as dramatically incorrect emission inventories) could be further verified and eventually incorporated into better emission parameterizations. Is the ABL budget method a practical technique for grounding-truthing regional emissions on a model-relevant scale?

We have add two paragraphs to the conclusions in order to suggest further research that may build on the accomplishments of this study.

Specific Comments

P2/L27: Wolfe et al. (2015) is another relevant and recent citation.

Thank you, yes, we have added that reference at this point. We had already included it in our paper elsewhere but had neglected it here.

Equations 4-7 and discussion thereof: Seems inconsistent. For example, the surface/entrainment terms are given different symbols for O3 and water. And the entrainment flux sign seems wrong – a higher concentration of stuff in the ABL should give rise to a positive entrainment flux (stuff leaving the ABL) and a negative contribution to dX/dt. It might be more straightforward to show a generic budget equation for any scalar, and then discuss specific treatments for water, ozone and methane.

You are correct, equation 4 had a sign inconsistency from our other equations, and there was substantial inconsistency in the symbols we had used. We have more systematically applied consistent symbols for the scalar budget equations and corrected the sign mistake. In response to a perceived misconception apparent in the reviewer's comment, we further added some discussion to clarify the role of entrainment in the ABL budget equations. A higher ABL concentration with everything else fixed would give rise to a dilution of the boundary layer concentrations, and yes this drives a negative dC/dt. However, this is not due to "stuff leaving the ABL" as the reviewer states. Entrainment in an actively turbulent ABL is an irreversible mixing process that incorporates free tropospheric (FT) air into the ABL, not vice versa. The positive scalar flux at the ABL top is the equivalent to a downward flux of concentration deficit (when the FT possesses a lower concentration), and we have explicitly stated that in the text now. We thank the reviewer for bringing this to our attention.

Page 8, Lines 16-22: suggest deleting.

Advice taken; we have removed these lines from the manuscript. We originally wanted to emphasize that in principal different scalars could be used in their respective budget equation to expose entrainment rates, i.e. water, ozone, or methane, and have made that point up front during the discussion of equations 4-7 as per reviewer's suggestions.

Eqn. 5: How are the BL concentrations determined for this calculation? Is it an average over the whole ABL, or just the upper portion? Same question for FT? Are uncertainties from this averaging (e.g. std of mean) propagated through to entrainment flux?

The scalar jump is determined from looking at vertical profiles and making the best eye judgment of the difference in concentrations between the top half of the ABL and the lowest ~100m of the FT. Often it is quite clear as can be seen in our example from fig. 7. We have included a brief description of how these values are determined and their estimated uncertainties, which are like all the terms propagated through to the final results. The error analysis section (4) has been greatly expanded so this should be much clearer now.

P12/L7: how is this map generated? Is it an interpolation of ground site data? Please expound. Also, another way of stating the opposing O3 and NO2 advective terms is that Ox=O3+NO2 is conserved.

The NOx and O3 advective maps are interpolated to a 2D grid from aircraft data taken in the ABL. All data is corrected for the calculated mean regional time rate of change back to a common time stamp of 13:30. This has been more clearly explicated in the text.

As for the odd oxygen interpretation, we do not agree. The gradient of ozone is an order of magnitude greater than that of NO_2. This is not simply a titration situation, but is intimately linked to rapid ozone production. We feel that the discussion of odd oxygen in this study would not serve to illuminate because it introduces a further unknown variable of the NOx emission rates. Also, we only had the NO_2 measurement on one single flight.

Section 3.2.3: These findings seem to suggest that NARR has serious flaws and should be adjusted, at least coarsely, to more accurately represent agricultural practices in some broad sense. A naïve question: would such issues impact the subsidence velocity derived from NARR?

We do not believe that large scale vertical motion would be all that susceptible to partitioning of surface heat fluxes among latent to sensible, but it certainly affects the convective activity and entrainment and boundary layer depths in the model. Subsidence is generally believed to be controlled by synoptic flow conditions. Although we do suspect that subsidence can modified a good bit due to mesoscale orography. A better representation of agricultural practices would lead to a better estimate of the latent heat flux, which affects the partitioning in the surface buoyancy flux, and for a constant net radiation forcing this would lead to lower ABL heights for greater latent heat fluxes. This is why the NARR ABL depths are so much higher than measured, for instance.

Table 3: The third column is technically not a flux, but a flux divergence. Also, please give CH4 production in ppmv/h for easy comparison with other terms.

The third column is the entrainment flux contribution to the flux divergence. We report it that way to have it in comparable units to the other terms. But reporting the surface emission similarly would not make sense to us, as the units most people

are familiar with are something like the chosen ones of Gigagrams per year. The CH4 production (surface emission) term is simply the numerical sum of the other columns, so we thought it would be redundant to see it in the same units.

Figure 9: is there any physical rationale behind a power-law fit?

The short answer is no. We know that the ozone chemistry is non-linear, and the simplest non-linear relationship is a power law.

Technical Comments

Fig. 2: Please label flight regions 1 and 2 as referenced in section 2.1.

We have changed the legend of Figure 2 to indicate the region numbers 1 and 2.

RASS is defined twice.

Got it.

P6/L32: delete ", which"

Deleted

P6/L35: "as per the Fundamental Theorem of Calculus" is a gratuitously pretentious statement.

We did not consider that such a foundational mathematical principle could be considered pretentious, but have eliminated the wording to protect the common reader.

Equations 1-3: subsidence is referred to as both $W(z_i)$ and W. Pick one.

Okay, thanks we will stick with just, W, with the implicit understanding that it can be a strong function of height.

P9, L13: delete "the 5 hour period of late morning to early afternoon from" P10/L17: delete "a remove of"

Done.

Referee #3

This paper describes the design and execution of two flight experiments in the San Joaquin Valley of California to quantify entrainment rates and then uses these entrainment velocities to solve for: (a) ozone production rates, (b) methane emissions, and (c) evapotranspiration. The authors are attempting numerous things here, which makes the paper difficult to read and, at times, the results difficult understand. The work is interesting, but paper would benefit from better organization around a clear goal prior to publication. Adding clarity may be as simple as removing the excessive inessential detail.

General comments:

The Introduction should be reorganized to better frame the work. Some specific issues are as follows.
In paragraph 2, the text does not define "tracer method" or "budget of the inversion base height" when describing what is done in the forthcoming analysis. This makes it difficult for the reader to know what is done here and how this work is different from past work.

We have added some clarification clauses to describe these methodologies, but exact details have to be postponed to the method descriptions of Section 2.

The sentence, "by way of targeted airborne campaigns we are able to probe the regional ABL vertically and horizontally and calculate entrainment rates and mesoscale advection," seems key, but is placed awkwardly in the middle of paragraph 3.

This statement is made after introducing the concepts of entrainment and advection, and therefore does not seem awkward in its placement to us. We have attempted to make a more clarion statement of the paper's overarching goal at the end of paragraph 3, keeping in mind that positional emphasis is typically carried by the end sentence of a paragraph (The Elements of Style, by Strunk & White [1999]):

> *The central goal of the work presented here is to show how, by way of targeted small-scale airborne campaigns, it is possible to probe the regional ABL vertically and horizontally to calculate entrainment rates and mesoscale advection, and thereby shed light on all of the processes that change the concentrations of trace gases in the boundary layer throughout the day. This methodology thereby reveals the quantitative origins of chemical constituents measured in near-surface air, by comparing direct observations of all but one of the leading terms of the scalar budget equation, and inferring the unknown term as a residual.*

The fourth paragraph returns to the idea of scalar budgeting, but still does not define, instead suggesting I should already be familiar with the concept (done through the particular way the references are discussed).

We have defined a scalar budget in an added subordinate clause in the second paragraph, and a new sentence at the end of the third paragraph as per earlier suggestions. Then we devote the entirety of Section 2.7 to defining exactly what the methodology is. We do not see how to further clarify the technique in the introduction without burdening the section with excessive detail.

While I agree with the content in paragraph 5, this paper is not actually about, "better understand[ing] the diurnal behavior of the wintertime boundary layer in the San Joaquin Valley."

We think that reporting observed entrainment rates in the winter, which have never been reported, does in fact help to better understand the ABL's diurnal behavior.

The discussion in paragraph 6 should more relevant to the analysis performed. For example, the paper never significantly discusses PM, but investigates ozone production, methane emissions, and evapotranspiration. While there is some text on ozone and drought here, methane is absent entirely.

We have added a concluding sentence to this paragraph that helps to establish the importance of the work:

> *Entrainment aloft becomes an even more important factor during stagnant conditions in the SJV because it represents the principal mode of ventilating the air pollutants in the ABL, and therefore its quantification is crucial to predicting the intensity and duration of an air quality episode.*

Although the work does not explicitly address PM issues, the results are directly applicable to the wintertime PM problem in the SJV and we hope will be used by others working on the DISCOVER-AQ data set. Also, because methane is not directly an air quality concern, we leave it out of this paragraph. We have removed a couple of sentences in the hopes that they might be considered "excessive inessential details."

The last paragraph presents an outline of the paper, but the preceding text has not setup these goals, nor does the outline mention the ozone production, methane emission, or evapotranspiration applications.

We have expanded the outline paragraph in an attempt to state the goals of our work more clearly, as per the reviewer's earlier suggestion.

Most of Section 2.1 is irrelevant. The authors should relate the descriptive information directly back to their analysis and delete superfluous detail.

We have condensed much of the information originally presented in Section 2.1 as it was also suggested by reviewer 2. However, we disagree that this discussion of the dynamic environment is irrelevant. We chose to include a clear survey of mountain-valley dynamics to set the stage for this unique mesoscale environment in which the experiments took place and because we do not find such a concise description anywhere in the extant literature. This dynamic complexity lies at the heart of why the region endures some of the poorest air quality in the nation. For others working on recalcitrant air quality issues in this area, or similar ones such as the Po Valley in Italy, we feel this information is essential for consideration.

Sections 2.6 and 2.7 should be framed around what was done here, rather than as done currently, as a general discussion of the two methods using the author's dataset as an example. The last sentence of Section 2.7, "ultimately the approach using the budget of boundary layer inversion height, outlined in Section 2.6 was taken to calculate the entrainment rate," should be given to the reader up front. Additionally, the last paragraph in 2.7 is described almost narratively of how the analysis was done. Please reorder such that results are presented to convey the logic of the analysis to the reader.

We have restructured/rewritten Section 2.7 to better coordinate the general discussion of the scalar budget equations with how they were used in these experiments.

What are the results for Ox, as opposed to O3 and NO2 separately? Use of P(Ox) would be especially important in the wintertime and better suited for a winter/summer comparison. Secondly, has wintertime P(O3) been found to be NOx-limited also? That seems unlikely; please clarify.

Unfortunately, we did not have measurements of NO_2 save for one single flight, and therefore were not able to perform a budget of odd oxygen.

- Yes, the results presented in Fig. 9 indicate that P(O3) is NOx-limited in the wintertime, but the inference is not strong given the limited spread in VOC:NOx ratio, and the uncertainties in using CH4 as a general VOC proxy. Nevertheless, we feel the result is worth presenting, especially since very little is known about winter O3 production because it is not often considered.

Broadly, the outline of the paper is to compute the entrainment rate and then use this rate to explore three things: (a) ozone production rates, (b) methane emissions, and (c) water. Adding text or a dedicated section after discussion of the three studies, but prior to the Conclusion, that ties everything back together would do two valuable things. First, it would clarify the narrative and logic of the paper, and second, it would reinforce the significance of the work.

We have attempted to tie everything together more clearly throughout the revised manuscript and thus do not see the value in repeating this before doing so again in the conclusions.

Specific comments:

Page 2, lines 3–4: Citation needed on, “this mixing tends to be a significant contributor to the ABL budget of the scalar.”

Stull [1990], Arellano et al. [2011], Lehning et al. [1998].

Page 3, lines 17–18: Should this be 105 exceedances "per year"?

We have eliminated this statement as non-essential.

Page 7, line 7: w(e) is not defined in the text (it is instead defined on page 8, line 23).

Defined in both places now.

Page 10, lines 18–20: What is the evidence for: “For the purposes of estimating regional source strengths or regional in situ photochemistry, we suggest that the more pertinent mixing process is the dilution of the anthropogenically influenced ABL air mass by the more global ’baseline’ FT air.”

This is more of a conjecture, claiming that it is the ABL growth rate after its initial ‘encroachment’ through the morning’s residual layer that is key in understanding regional chemistry and surface emissions because the residual layer tends to be made up of mostly recycled air from the region. Of course, in principle, the budgets should still hold during the more rapid growth of the morning ABL, but they become more difficult to accurately measure due to the greater presence of transients and inhomogeneities. We do not feel this detail should be introduced into the manuscript because it is somewhat tangential as we did not perform the budget analysis in the morning hours, and it would not make sense to anyway because of the low O3 production at high solar zenith angles, which does not impact the afternoon O3 maximum very significantly.

Page 11, lines 34–35: How is this shown in Fig. 7: “the importance of entrainment mixing on an ozone exceedance day.”

It is shown in the subsequent discussion where the jumps observed in Fig. 7 are used to estimate a time rate of change of O_3 and NO_2 concentrations due to entrainment dilution.

Page 12, lines 35–36: It is difficult to see that methane is an appropriate proxy for total VOC. Even if dairies and gas production are the dominant source of VOCs, what

matters more is that the drivers of methane emission match the drivers of the other VOC, which might not be true even if the sources are the same.

As discussed in Section 3.2.2 the majority of methane in both studies are believed to be associated with fossil fuel extraction and dairy operations. The studies of Gentner et al. [2014] and Pusede et al. [2014] indicate that methane is fairly well correlated with alcohols (which have strong dairy sources), higher alkanes (natural gas), and CO (other anthropogenic activities.) While we acknowledge that methane is a somewhat crude tracer of reactive VOC, we present the results because there is a suggestive relationship with our inferred ozone production rates that is consistent with past studies of the ozone production regime.

Page 13, lines 3–5: Can an estimate of the uncertainty be given?

We have included an average uncertainty estimate from our experimental results to better frame the comparison, and have done so in all of the Tables as well. There is no estimate of uncertainty in P(O3) made by Pusede et al. (2014).

Section 4: I recommend moving Section 4 to precede Sections 3.2.1–3.2.3.

We feel that a discussion of the errors in the measurements specifics is best delayed until the details of the experimental results are related, so we have kept Section 4 after Section 3, but we have expanded it considerably to make clear exactly how our errors have been treated in our results.

Interactive comment on Atmos. Chem. Phys. Discuss., doi:10.5194/acp-2016-635, 2016.

Observing Entrainment Mixing, Photochemical Ozone Production, and Regional Methane Emissions by Aircraft Using a Simple Mixed-Layer Model

Justin F. Trousdell[1], Stephen A. Conley[1,2], Andy Post[*], Ian C. Faloona[1]

[1]Department of Land, Air, and Water Resources, University of California Davis, United States
[2]Scientific Aviation, Inc., Boulder, Colorado, United States
*now at the California Air Resources Board, Sacramento, California, United States

Correspondence to: Ian C. Faloona (icfaloona@ucdavis.edu)

Abstract. In situ flight data from two distinct campaigns during winter and summer seasons in the San Joaquin Valley (SJV) of California are used to calculate boundary layer entrainment rates, ozone photochemical production rates, and regional methane emissions. Flights near Fresno, California in January and February 2013 were conducted in concert with the NASA DISCOVER–AQ project. The second campaign (ArvinO3), consisting of eleven days of flights spanning June through September 2013 and in June 2014 focused on the southern end of the SJV between Bakersfield and the small town of Arvin, California, a region notorious for frequent violations of ozone air quality standards. Entrainment velocities, the parameterized rates at which free tropospheric air is incorporated into the atmospheric boundary layer (ABL), are estimated from a detailed budget of the inversion base height. During the winter campaign near Fresno, we find an average midday entrainment velocity of 1.5 cm s^{-1}, and a maximum of 2.4 cm s^{-1}. The entrainment velocities derived during the summer months near Bakersfield averaged 3 cm s^{-1} (ranging from 0.9 – 6.5 cm s^{-1}), consistent with stronger surface heating in the summer months. Using published data on boundary layer heights we find that entrainment rates across the Central Valley of California have a bimodal annual distribution peaking in spring and fall when the lower tropospheric stability (LTS) is changing most rapidly.

Applying the entrainment velocities to a simple mixed–layer model of three other scalars (O_3, CH_4, and H_2O), we solve for ozone photochemical production rates and find wintertime ozone production (2.8 ± 0.7 ppb h^{-1}) to be about one-third as large as in the summer months (8.2 ± 3.1 ppb h^{-1}). Moreover, the summertime ozone production rates observed above Bakersfield/Arvin exhibit an *inverse* relationship to a proxy for the VOC:NO_x ratio (aircraft [CH_4] divided by surface [NO_2]), consistent with a NO_x–limited photochemical environment. A similar budget closure approach is used to derive the regional emissions of methane, yielding 100 Gg yr^{-1} for the winter near Fresno and 170 Gg yr^{-1} in the summer around Bakersfield. These estimates are 3.6 and 2.4 times larger, respectively, than current state inventories suggest. Finally, by performing a boundary layer budget for water vapour, surface evapotranspiration rates appear to be consistently ~55% of the reference values reported by the California Irrigation Management Information System (CIMIS) for nearby weather stations.

1 Introduction

During the daytime over the continents, when ozone (O_3) reaches its peak, convective thermals generated by surface heating rise and penetrate into the stable layer that demarcates the interface between the turbulent atmospheric boundary layer (ABL) and the laminar (non–turbulent) free troposphere (FT) above it. The continuous action of these thermals penetrating into the laminar overlying air and falling back into the boundary layer gives rise to an irreversible mixing process that causes the layer to grow up

Ian Faloona 9/14/2016 12:35 AM
Deleted: at the surface

through the mid–morning to afternoon, diluting the air in the ABL with that from the FT. The overall process is referred to as entrainment, and when the two layers contain different amounts of any scalar quantity (e.g. ozone concentration, water vapour, enthalpy), this mixing tends to be a significant contributor to the ABL budget of the scalar (Arellano et al., 2011; Lehning et al., 1998), and therefore vital to predicting and interpreting its abundance at the surface.

Typically entrainment is not treated explicitly in chemical transport models because the scales of motion, taking place predominantly within the ABL capping inversion, are suppressed in vertical extent due to the thermodynamic stability of this layer. Consequently the mixing tends to be sub–grid in nature and requires some form of parameterization. Many aircraft measurements of this parameter have been attempted using the tracer method (Nichols, 1984; Kawa & Pearson, 1989; Faloona et al., 2005; Karl et al., 2013) wherein a trace gas flux is divided by the jump in its concentration across the inversion, however this requires the use of eddy correlation to measure the turbulent fluxes near the top of the ABL. Because the aircraft used in the present study, operated by Scientific Aviation, Inc., does not currently have the capability to measure vertical wind speeds, we use here instead measurements of the ABL growth rate and a budget of the inversion base height (Wood & Bretherton, 2004; Faloona et al., 2005; Albrecht et al., 2016) to infer the entrainment rate based on the fact that ABL growth is driven in large part by entrainment.

Another meteorological process that can strongly influence surface concentrations is horizontal advection, and owing to the intricacies of the surface wind field in complex terrain and heterogeneity of surface sources of trace gases, this term has traditionally been difficult to account for in ground–based air pollution studies. Past measurements of DMS, SO_2, and O_3 budgets carried out over the (presumed homogenous) ocean indicate that while on average the advection term is not large, it can be dominant on any given day, and so must be considered when looking at individual episodes (Conley et al., 2009; Faloona et al., 2010; Conley et al., 2011). The central goal of the work presented here is to show how, by way of targeted small-scale airborne campaigns, it is possible to probe the regional ABL vertically and horizontally to calculate entrainment rates and mesoscale advection, and thereby shed light on all of the processes that change the concentrations of trace gases in the boundary layer throughout the day. This methodology thereby reveals the quantitative origins of chemical constituents measured in near-surface air, by comparing direct observations of all but one of the leading terms of the scalar budget equation, and inferring the unknown term as a residual.

Outlined in the seminal work of Lenschow et al. (1981) are original applications of the scalar budgeting techniques used by Warner & Telford (1965) and Lenschow (1970) to help validate the newly developing technique of eddy covariance for measuring sensible heat fluxes by aircraft. Lenschow et al. (1981) go on to describe the effectiveness of well-designed aircraft ABL studies in determining the net source or sink (in their case for ozone) given the careful measurement of the other dynamically controlled terms. The technique can be generalized to any scalar budget (i.e. ozone, water vapour, DMS, SO_2, and isoprene) to enable the calculation of important residuals including source or sink terms for non–conserved species (Kawa & Pearson, 1989; Bandy et al., 2012; Conley et al., 2009; Faloona et al., 2010; Wolfe et al. 2015). In the process of quantifying the individual terms of the budget equations, their relative importance can be weighted to provide a better understanding of the leading causes and factors affecting surface concentrations.

A contemporary challenge for air quality monitoring in the age of increasing sophistication of remote sensing from space is correlating surface concentrations of key trace gases (ex. NO_x, O_3, etc.), with column measurements from satellite. Many air pollutants of interest are concentrated predominantly in the boundary layer, where the main sources are often located, thus there

Ian Faloona 9/14/2016 12:37 AM
Deleted: atmospheric boundary layer (

Ian Faloona 9/14/2016 12:37 AM
Deleted:)

Ian Faloona 9/14/2016 12:38 AM
Deleted: free troposphere

Ian Faloona 9/14/2016 12:39 AM
Deleted: process

Ian Faloona 9/14/2016 12:10 AM
Deleted: base

Ian Faloona 9/14/2016 12:10 AM
Deleted: inversion

Ian Faloona 9/14/2016 12:13 AM
Deleted: .

Ian Faloona 9/14/2016 12:31 AM
Deleted: mesoscale

Ian Faloona 9/18/2016 1:50 PM
Deleted: complexity

Ian Faloona 9/18/2016 1:15 PM
Moved down [4]: By way of targeted airborne campaigns we are able to probe the regional ABL vertically and horizontally and calculate entrainment rates and mesoscale advection. This flight strategy thus helps to illuminate the origins of surface levels of various chemical constituents, by comparing the observations, including the rate of advection, with the overall scalar budgeting equation.

Ian Faloona 9/14/2016 12:28 AM
Deleted: ably

Ian Faloona 9/18/2016 1:15 PM
Moved (insertion) [4]

Ian Faloona 9/18/2016 1:38 PM
Deleted: B

Ian Faloona 9/18/2016 1:51 PM
Deleted: we are able

Ian Faloona 9/18/2016 1:39 PM
Deleted: and

Ian Faloona 9/18/2016 1:43 PM
Deleted: flight strategy thus

Ian Faloona 9/18/2016 1:43 PM
Deleted: helps to illuminate

Ian Faloona 9/18/2016 1:44 PM
Deleted: the

Ian Faloona 9/18/2016 1:40 PM
Deleted: surface levels of various

Ian Faloona 9/18/2016 1:42 PM
Deleted: the

Ian Faloona 9/18/2016 1:47 PM
Deleted: , including the rate of advection, with the overall

Ian Faloona 9/18/2016 1:41 PM
Deleted: ing

Ian Faloona [2] 9/12/2016 12:38 PM
Deleted:)

is a strong need for understanding the diurnal behaviour of the mixed layer. One possible way to improve the correlation between surface and column concentrations is by understanding its connection to ABL height, and also the role of ABL mixing with the FT (entrainment). The depth of the ABL directly affects the concentration of tracers (i.e. surface levels), as they will be diluted and mixed throughout it. Recent studies in California by Al−Saadi et al. (2008) suggest that lidar measurements of ABL height can normalize column observations of AOD (Aerosol Optical Depth) to greatly improve correlations to surface PM2.5 (Particulate Matter up to 2.5 micrometers in size). Improving the inference of surface concentrations from satellite data is among the chief scientific goals of the NASA experiment DISCOVER–AQ (Deriving Information on Surface Conditions from COlumn and VERtically Resolved Observations Relevant to Air Quality). Seven of our flights were conducted during the California campaign of DISCOVER–AQ, in an effort to support their scientific mission. DISCOVER–AQ sought to use concurrent integrated observations to meet this goal, among them was the University of California Davis (UC Davis) in situ aircraft measurements of trace gas, and thermodynamic budgets to better understand the diurnal behaviour of the wintertime boundary layer in the San Joaquin Valley.

The San Joaquin Valley (SJV) of California is well known for its ozone (summer) and PM2.5 (winter) air quality challenges. As of 2013 the Valley is a non-attainment site for the state standard and the federal 8-hour standard for O_3, a status that is likely to only become aggravated by the recent reduction in the federal 8h standard to 70 ppbv (US EPA). Additionally, the majority of the SJV, especially the southern portion, is designated non-attainment for PM2.5 for state and federal standards (California Air Resources Board (CARB)) as of 2013. In winter the SJV is plagued by PM2.5 problems related to strong temperature inversions, low mixed layer heights, and more recently extreme drought conditions. In the southern SJV weak surface winds and a unique basin topography add to the problem of stagnation and, in general, a strong temperature inversion exists aloft over the entire SJV restricting the convective venting of pollution. Entrainment aloft becomes an even more important factor during stagnant conditions in the SJV because it represents the principal mode of ventilating the air pollutants in the ABL, and therefore its quantification is crucial to predicting the intensity and duration of an air quality episode.

Here we will present the results of two flight campaigns targeting the SJV in winter and summer, and show the utility of applying simple mixed-layer budget equations to airborne measurements in order to calculate entrainment velocities, and then apply these to get the entrainment rates of three trace gases: O_3, CH_4, and water vapour. With the additional measurements of these species' temporal trends and horizontal advection rates, important budget residuals are deduced such as O_3 photochemical production, regional methane emissions, and latent heat fluxes. First we turn to a discussion of the uniqueness of the SJV including the synoptic setting as well as the important mesoscale features. Then we describe the measurements used in the analysis along with the methods of ABL budgeting. In Section 3 we discuss the results from the analysis, provide a thorough assessment of the probable errors in the results in Section 4, and make some suggestions for further applications in our conclusions reviewed in Section 5.

2 Experimental Description

2.1 Synoptic and Geophysical Setting

The arid weather experienced throughout most of California during the summer is under the weight of the prevailing Pacific High, centred near 35° N some 2000 km offshore (Fig. 1 bottom right), which blocks storm systems from hitting the state instead shunting them northward towards Canada. The domineering anticyclone also drives synoptic scale subsidence on its downwind

Ian Faloona 9/19/2016 1:16 AM
Deleted: only going

Ian Faloona 9/19/2016 1:18 AM
Deleted: ing

Ian Faloona 9/19/2016 1:03 AM
Deleted: .

Ian Faloona 9/19/2016 1:02 AM
Deleted: Although more dominant during t ... [1]

Ian Faloona 9/19/2016 1:03 AM
Deleted: vertical motions and

Ian Faloona 9/19/2016 1:18 AM
Deleted: High temperatures in summer cou ... [2]

Ian Faloona 9/19/2016 1:48 AM
Deleted: discuss

Ian Faloona 9/19/2016 1:48 AM
Deleted: the

Ian Faloona 9/19/2016 1:55 AM
Deleted: efficacy

Ian Faloona 9/19/2016 1:52 AM
Deleted: using

Ian Faloona 9/19/2016 1:50 AM
Deleted: d

Ian Faloona 9/19/2016 1:50 AM
Deleted: regional

Ian Faloona 9/19/2016 1:53 AM
Deleted: rates

Ian Faloona 9/19/2016 1:58 AM
Deleted: w

Ian Faloona 9/19/2016 1:54 AM
Formatted ... [3]

Ian Faloona 9/19/2016 1:54 AM
Formatted ... [4]

Ian Faloona 9/19/2016 2:02 AM
Deleted: known budget terms in exposing

Ian Faloona 9/19/2016 2:02 AM
Deleted: like methane emissions and in situ

Ian Faloona 9/19/2016 2:03 AM
Deleted: will start by

Ian Faloona 9/19/2016 2:03 AM
Deleted: ng

Ian Faloona 9/19/2016 2:03 AM
Deleted: flight regions

Ian Faloona 9/19/2016 2:05 AM
Deleted: The next section will

Ian Faloona 9/19/2016 2:05 AM
Deleted: detail our mixed layer model, foll ... [5]

Ian Faloona 9/19/2016 2:09 AM
Deleted: including budget residuals and fi ... [6]

Ian Faloona 9/19/2016 1:32 AM
Deleted: s

Ian Faloona [2] 9/9/2016 12:52 PM
Deleted: moreover

flank over the region. A strong thermodynamic "lid" or temperature inversion is set up by the synoptic subsidence, which resists convective motions throughout the lower atmosphere, leading to the collaboration of stagnant horizontal winds, sunny skies, and reduced vertical mixing that is emblematic of ozone pollution episodes. The zonal pressure gradient and surface friction impel a degree of onshore flow (atmospheric Ekman transport) that is principally blocked by the coastal mountains. The low–level summertime airflow into the interior of the state is therefore restricted to the main break in the Coast Range near the San Francisco Bay area and is strengthened by the land–ocean thermal contrast, with air entering the Carquinez Strait just beyond the San Francisco Bay and diverging into the conjoined Sacramento and San Joaquin Valleys that together make up the great Central Valley of California (Schultz et al. 1961; Frenzel 1962; Hays et al. 1984; Moore el al. 1987; Zaremba and Carroll 1999). This restricted airflow is the feedstock of the Central Valley air and is diverted northwest into the Sacramento Valley and southeast into the San Joaquin Valley as it butts up against the tall Sierra Nevada mountain. The SJV is flanked by three mountain ranges - the Southern Sierra Nevada mountains to the east, the Tehachapi mountain range south, and to the west the Pacific Coast Range - limiting outflow and ventilation and leading to orographic stagnation and uplift towards the southern end of the valley. However, airflow at higher elevations over the valley air and surrounding mountains is entrained down into the valley boundary layer due to convective turbulent mixing during the daytime. It is precisely this mixing mechanism that is critical to understanding the set-up and evolution of air pollution events in the valley, and what we set out to quantify in this study.

In the SJV a nonlinear superposition of flows dictates the observed winds. In addition to the synoptic forcing discussed above, there is a direct thermal forcing of the mountain-valley circulation with consequent up-slope flows inducing mesoscale subsidence over the central valley floor (Rampanelli et al., 2004; Shcmidli & Rotunno, 2010). In the far southern end of the San Joaquin up-valley air is forced to converge as it runs into the steep topography of the Tehachapi Mountains. This low-level orographic convergence, which was shown in ABL wind data by Bianco et al. (2011), gives rise to mesoscale uplift especially pronounced at the cul-de-sac of the valley. Monthly composites of vertical velocity (omega) from the National Center of Environmental Prediction/North American Regional Reanalysis (NCEP/NARR) dataset, averaged over the decade from 2004 to 2013, are depicted in Figure 1. Upward motion is present across large swaths of the Central Valley during summer, likely due to orographic lift on the windward side of the Sierras, but it appears especially strong in the southern end of the valley (Fig. 1) where the thermal valley wind and southern mountains augment the effect.

The complex mesoscale terrain plays a very important role in the valley atmosphere. The influence of topography on the thermally driven flow pattern arising from land–ocean contrast in the California Central Valley during the summer is discussed in Zhong et al. (2004). Their study employed the use of 22 wind profilers with radio acoustic sounding systems (RASS) to vertically probe the atmosphere. The authors suggest, based on temperature profiles in the lowest 800 m, that the mixed layer height, which probably exceeds 1000 m AGL, slopes up valley in the San Joaquin. Additionally, the thermally driven flow pattern frequently extends upward to 800–1000 m AGL. Bianco et al. (2011), investigating various factors influencing ABL height in the Central Valley, reported low–level convergence in the southern end of the valley leading to increased ABL heights. They did so by looking at the difference in up–valley wind between two sites in the SJV, Chowchilla and Lost Hills. This is in contrast to sites to the north in the SJV which see a shoaling in the summer months, likely due to cold air advection from the coast, or subsidence induced from the valley flow (far from the cul-de-sac at the Tehachapi Mountains), or possibly other causes such as land use, wherein different irrigation patterns may lead to a different partitioning of latent and sensible heat fluxes. Our study corroborates the convergence in the southern end of the valley in that the NCEP/NARR reanalysis data set shows strong

Ian Faloona [2] 9/9/2016 3:52 PM
Deleted: ,

Ian Faloona [2] 9/9/2016 3:52 PM
Deleted: ing

Ian Faloona [2] 9/9/2016 12:53 PM
Deleted: . This is why the state experiences a long dry, hot and sunny summer

Ian Faloona [2] 9/9/2016 3:54 PM
Deleted: around

Ian Faloona [2] 9/9/2016 12:59 PM
Deleted: v

Ian Faloona [2] 9/9/2016 12:56 PM
Deleted: e

Justin 8/24/2016 3:47 PM
Comment [1]: I think that we could do away with most of this paragraph honestly, we wouldn't lose much. I will leave it up to you to cut it or not.

Ian Faloona [2] 9/9/2016 12:51 PM
Deleted: range on the far side of the Central Valley and large scale vertical motions are generally suppressed due to the stable subsidence inversion above

Ian Faloona [2] 9/9/2016 5:02 PM
Moved (insertion) [1]

Ian Faloona [2] 9/9/2016 5:02 PM
Deleted: n

Ian Faloona [2] 9/9/2016 5:02 PM
Deleted: , and needed to be taken into consideration for this study

uplift at the southern extremity of the SJV, and that there is often an unmistakable decrease in meridional winds approaching the southern mountains observed by the aircraft winds (data not shown.)

Seven flights from 16 January to 4 February of 2013 were deployed across the San Joaquin valley transverse to its axis with extensive vertical profiling of the ABL and the free troposphere (FT) above it, in conjunction with the NASA DISCOVER–AQ California campaign (flight region 1, see Fig. 2). In each vertical profile up and down through the ABL we monitored the inversion height in addition to a suite of scalar measurements (ozone, water vapour, methane, horizontal winds, carbon dioxide, and temperature). In addition, on each profile we fly up through the ABL top in order to characterize the composition and thermodynamic properties of the FT. The second set of deployments was focused at the southern end of the SJV during the summer months employing a slightly different flight strategy (flight region 2, see Fig. 2). Although vertical probing up and out of the ABL was consistent, a greater emphasis was placed on the horizontal extent of the measurements in the direction of the mean ABL wind. The main focus of this campaign was to better understand the cause of the large number of ozone NAAQS exceedances in this region surrounding the small town of Arvin. To do so required a thorough quantification of the horizontal advection as well the entrainment flux of O_3 (directly related to entrainment rates). Flights were targeted at O_3 exceedance episodes with each of four deployments lasting 2–3 days spanning two summers (2013-2014) between June and September.

2.2 Aircraft Measurements

Our flight data was collected aboard a single engine Mooney TLS, operated by Scientific Aviation, Inc. (http://www.scientificaviation.com), and piloted by one of the authors (SC). The Mooney is outfitted with a 2B Technologies O_3 monitor, a Vaisala HMP60 temperature and Relative Humidity probe, a modified Picarro 2301f Cavity Ring–Down Spectrometer (CRDS) to measure CO_2, CH_4, and H_2O, and an Aspen Avionics PFD1000 flight display delivering pressure, altitude, true air speed, etc. Measurement of the horizontal wind is accomplished using a novel technique developed for easy and inexpensive deployment on a single engine aircraft. Utilizing a dual GPS antenna to provide accurate airplane heading and a ground velocity by vector subtraction from true air speed (TAS) the horizontal wind is calculated, a technique outlined in Conley et al. (2014).

2.3 Sortie Strategies

In order to support the objectives of the DISCOVER–AQ campaign by probing the boundary layer dynamics near the northern edge of the domain, the aircraft was flown back and forth perpendicular to the valley axis approximately between the NASA profile stations at Fresno and Tranquility (Fig.2). In the absence of making fast vertical wind measurements, we derive entrainment rates in a novel way using a complete scalar budget of the ABL height throughout each flight targeted from midday to late afternoon hours (usually 11:00–16:00 PST). The flight hours are specifically chosen to focus on the ABL dynamics after its initial, rapid growth through the residual layer in the mid-morning. The inferred entrainment rates derived from the ABL height–budget, are then used in all of the scalar budgets to reveal O_3 photochemical production rates, surface latent heat fluxes, and regional methane emissions as residuals.

To study the processes that govern the evolution of the surface concentration of O_3 during the summer months in the southern SJV more in-depth, we performed an airborne experiment in collaboration with Scientific Aviation, Inc. targeting the vicinity of Arvin, California during the summers of 2013 and 2014. Flying around and upwind of Arvin 3–7 hours per day during each of

Ian Faloona [2] 9/9/2016 12:50 PM
Deleted: As the evening progresses down–slope, katabatic flows, which are strongest on the flanks of the highest parts of the Sierra Nevada range to the east, interact with the valley wind, taking the form in the evening of a low–level jet, and giving rise to a mesoscale, cyclonic circulation referred to as the Fresno Eddy (Lin & Jao, 1995; Zhong et al., 2004; and Bao et al., 2008). The Fresno Eddy is most pronounced in the early morning as a combinatory effect of the up–valley low–level jet, which peaks before midnight and the southeasterly down–slope flow strengthening throughout the night until sunrise.

Justin 8/24/2016 3:40 PM
Deleted: : measuring the difference in a scalar quantity from a well–mixed layer to the FT is essential to understanding entrainment fluxes

Ian Faloona [2] 9/9/2016 5:05 PM
Deleted:

Ian Faloona [2] 9/9/2016 5:02 PM
Moved up [1]: The complex mesoscale terrain plays an important role in the valley atmosphere, and needed to be taken into consideration for this study. The influence of topography on the thermally driven flow pattern arising from land–ocean contrast in the California Central Valley during the summer is discussed in Zhong et al. (2004). Their study employed the use of 22 wind profilers with radio acoustic sounding systems (RASS) to vertically probe the atmosphere. The authors suggest, based on temperature profiles in the lowest 800 m, that the mixed layer height, which probably exceeds 1000 m AGL, slopes up valley in the San Joaquin. Additionally, the thermally driven flow pattern frequently extends upward to 800–1000 m AGL. Bianco et al. (2011), investigating various factors influencing ABL height in the Central Valley, reported low–level convergence in the southern end of the valley leading to increased ABL heights. They did so by looking at the difference in up–valley wind between two sites in the SJV, Chowchilla and Lost Hills. This is in contrast to sites to the north in the SJV which see a shoaling in the summer months, likely due to cold air advection from the coast, or subsidence induced from the valley flow (far from the cul-de-sac at the Tehachapi Mountains), c ... [7]

Justin 8/24/2016 3:47 PM
Comment [2]: I think that we could do away with most of this paragraph honestly, we wouldn't lose much. I will leave it up to you to cut it or not.

Ian Faloona [2] 9/9/2016 1:02 PM
Deleted: The SJV is flanked by three mountain ranges: the Sierra Nevada mountain range to the east, the Tehachapi mountain range south, and the Pacific Coast Ranges to the west. Winds within a mountain–valley system are observed to exhibit a diurnal pattern; up–slope and up–valley flow during the day and down–slope and down–valley flow at night. Drivers for mountain–valley flows are usuall ... [8]

Justin 8/24/2016 1:12 PM
Deleted: The maximum is reached when the ageostrophic wind component aligns with up-valley flow before midnight, the result of an inertial oscillation (Zhong et al. 2004) in response to the decoupling of ABL winds from the surface after sunset. Zhong et al. (2004) estimates the phase difference, or response time, between the along valley wind and the along valley pressure gra ... [9]

the four 3 day campaigns, observations of wind, temperature, methane, water vapour, and ozone were used to measure the principal dynamical components of the total ozone budget: namely, advective up–valley transport within the ABL and entrainment mixing from above. By comparing these measured dynamical terms with the observed O_3 rise throughout the region during the afternoon, and using a reasonable parameterization of dry deposition, the net photochemical production rate can be inferred. Consequently, the relative contributions of these processes to the resulting surface O_3 concentration can be estimated for midday conditions, which are most important in determining whether an ozone exceedance of the NAAQS is reached. On one of the flights during the second deployment (15 August 2013) we additionally made NO_2 measurements with a Los Gatos Research cavity enhanced absorption spectrometer. All flights, for both campaigns, targeted days with weak horizontal winds in the ABL because stagnation tends to accompany both wintertime PM2.5 and summertime O_3 episodes.

2.4 NARR Data

Because we are not able to accurately measure mean vertical wind speeds by aircraft currently, we resort to the NCEP NARR dataset to estimate the mean vertical wind speed at the top of the ABL during each flight. NARR is an extension of the NCEP global reanalysis, and was created to provide long–term consistent climate data focused over the U.S. at a regional scale. The model runs at 32 km resolution with 45 vertical layers providing data eight times a day with a reanalysis period from 1979–2015. More information about this reanalysis data set can be found at http://www.esrl.noaa.gov/psd/data/gridded/data.narr.html.

2.5 NOAA Sounding System Data

We make heavy use of the data collected by NOAA during 2008 from five 915 MHz radar wind profilers equipped with radio acoustic sounding systems (RASS) distributed across the Central Valley and reported in Bianco et al. (2011). Briefly the radio signal backscatter is augmented in regions with strong fluctuations in temperature and water vapour as exists in the entrainment zone at the top of the ABL. The method of Bianco et al. (2008) uses not only the backscattered intensity, but further includes the vertical velocity variance and its spectral width to automatically select the ABL top throughout the day. The minimum gate height for these profilers is 120–140 m above ground, and their vertical resolution is 60 m. To evaluate the average ABL growth rates we simply subtract the mean height at 11:00 from 15:00 and divide by the 5 hour interval.

2.6 Budget of the ABL Inversion Height

Quite often the growth rate of the boundary layer is interpreted as equivalent to the entrainment velocity, w_e, or volume flux of FT air into the ABL (Tennekes 1973), assuming that there is no large scale mean vertical wind. However, in most situations the ABL growth ($\frac{dz_i}{dt}$) is actually determined by the difference of two distinct processes: the entrainment, which is considered to be driven by micrometeorological factors (viz. surface buoyancy flux, inversion strength, and possibly wind shear across the inversion), and the larger scale subsidence, W, in the lower FT just above the ABL, which is forced by synoptic flow patterns.

$$w_e = \frac{dz_i}{dt} - W \quad (1)$$

In a seminal paper on the effects of surface heating on the inversion height, Ball (1960) declared that there are several processes that counteract the tendency of entrainment to raise the inversion height. One is that "horizontal divergence in the lower layers, accompanied by subsidence at inversion level, may be sufficient to counteract the rise", and the other is that the "inversion usually slopes upward along the trajectories and thus advection tends to lower the inversion at a fixed point." To be even more

Ian Faloona 9/13/2016 10:41 PM
Deleted: ,

Ian Faloona 9/14/2016 1:33 AM
Formatted: Font:Italic

Ian Faloona 9/14/2016 1:33 AM
Formatted: Font:Italic, Subscript

Ian Faloona 9/13/2016 10:19 PM
Formatted: Font:Italic

Ian Faloona 9/13/2016 10:17 PM
Deleted: (*W*

Ian Faloona 9/13/2016 10:18 PM
Deleted:)

precise we consider the total derivative of the ABL or mixed layer height (z_i) and expand it into the Eulerian derivative of ABL height and an advection term. The resultant z_i budget equation leads to a relationship between the entrainment velocity, the observed local ABL growth rate, the mean advection of ABL depth, and the mean vertical velocity at the inversion height:

$$w_e = \frac{\partial z_i}{\partial t} + U\frac{\partial z_i}{\partial x} - W \quad (2)$$

The first two terms on the right hand side of Eq. (2) are, in principle, easily observed by aircraft, while the last term has evaded careful measurement by aircraft or any other means (Lenschow et al., 1999; Angevine 1997; Lenschow et al., 2007). While the sorties provided a sufficient number of ABL crossings to estimate the ABL growth rate with acceptable accuracy, there were generally not enough at different locations to capture an unbiased, two-dimensional gradient of the inversion height (second term on the rhs of Eq. 2). Consequently, we estimate the advection term using the gradient in ABL height as determined from the NCEP/NARR data set in conjunction with the observed in situ mean wind (Fig. 3). The observations of z_i indicate that the reanalysis data does not predict the absolute boundary layer depth with great accuracy in the Central Valley. This is most likely due to the fact that the model does not treat the heavily irrigated agricultural land surface with any fidelity. Inspection of the surface latent heat fluxes in the model (data not shown) indicate unrealistically small values for a region with such fecund agricultural productivity. Nevertheless, we assume here that the reanalysis data does capture the gradients of ABL depth reasonably well. In fact, the gradients evinced in Fig. 3 are in rough accord with those reported in Bianco et al. (2011), approximately 500 m difference across the lower ~200 km of the southern SJV. The large–scale vertical mean wind, W, is derived from the NCEP/NARR pressure velocity omega ($\omega = \frac{dp}{dt}$), and the surface pressure tendency neglecting horizontal pressure advection and assuming hydrostatic balance:

$$W = \frac{1}{\rho g} * \left(\frac{\partial p}{\partial t} - \omega\right), \quad (3)$$

The pressure level from which to select the omega value was chosen using the hypsometric equation $\left(p_2 = p_1 * \exp\left(-\frac{z_i * g}{R_d * \bar{T}}\right)\right)$ using an average observed ABL height, z_i, an average ABL temperature, $\bar{T}$, for the flight duration, R_d is the dry air gas constant, and an estimated average surface pressure, p_1, of 1010.5 mb for June–Sept, and 1020 mb for Jan–Feb.

The local pressure change is estimated by the surface pressure tendency using hourly data from several CARB (The California Air Resources Board: http://www.arb.ca.gov/aqmis2/metselect.php) meteorology stations in the area over the flight time. Throughout the afternoon during both seasons the valley experiences a fairly strong and consistent drop in surface pressure of approximately 0.6 mb h^{-1}. Similar diurnal oscillations of surface pressure were found by Li et al. (2009) to be prevalent in deep mountain valleys of the western US. Although these pressure changes are large by synoptic standards, they are generally an order of magnitude smaller than the omega values.

2.7 Mixed Layer Model

Ultimately the estimation of the entrainment rate made by applying Eq. 2 to the aircraft measurements and reanalysis data is used to illumine the specifics of trace gas evolution by connecting it to their individual entrainment rates in each one's own budget equation. For example, the scalar budget of ozone in a well-mixed ABL can be mathematically represented as:

$$\frac{\partial O_3}{\partial t} = -U\frac{\partial O_3}{\partial x} + \frac{(w'O_3')_s - (w'O_3')_{z_i}}{z_i} + P \quad (4)$$

Ian Faloona 9/17/2016 11:42 PM
Deleted: $-\frac{\partial p}{\partial t}$

Ian Faloona 9/18/2016 12:50 AM
Moved (insertion) [3]

Ian Faloona 9/18/2016 12:51 AM
Deleted: approach using the budget of boundary layer inversion height, outlined in Section 2.6 was

Ian Faloona 9/18/2016 12:58 AM
Deleted: taken to calculate the entrainment rate

Ian Faloona 9/18/2016 12:58 AM
Deleted: Briefly, the

Ian Faloona 9/18/2016 12:59 AM
Deleted: ozone

Ian Faloona 9/18/2016 12:59 AM
Deleted: the

Ian Faloona [2] 9/12/2016 1:49 PM
Deleted: –

Ian Faloona [2] 9/12/2016 1:42 PM

Ian Faloona [2] 9/12/2016 1:56 PM
Deleted: $+F_{ent}$

Ian Faloona [2] 9/12/2016 5:38 PM
Deleted: ,

The first term on the left represents the observed temporal trend in a fixed region, the second term represents the advection (the influence of the mean wind, U, acting on the ~~mesoscale gradient in the O_3 field~~), z_i is the ABL depth, ~~the third term is the opposite of the vertical turbulent flux divergence, and P represents the net photochemical production (Conley et al., 2011).~~ We use observations/estimates of the first four terms of Equation 4 to solve for the net production rate of ozone. The surface flux, F_{s_2}, for a reactive species like ozone that is taken up in plant stomata is parameterized as the product of a deposition velocity, v_{dep}, and mean concentration, $F_s \equiv (w'O_3')_s \cong -v_{dep}[O_3]$. ~~The entrainment flux, F_{ent}, on the other hand, is due to mixing in of free~~ tropospheric air at the top of the ABL, and is commonly parameterized as the product of the entrainment velocity of Equations 1 & 2, and the concentration difference (or scalar jump) across the inversion interface at z_i, $F_{ent} \equiv (w'O_3')_{z_i} \cong -w_e\Delta[O_3]_{FT-ABL}$. This relationship applies to all the scalars and thus the determination of w_e feeds into each budget equation.

The scalar jumps are diagnosed from vertical profiles made during each flight (see Fig. 7 for an example). From experience, we have found it best not to attempt its determination with an algorithm, and instead calculate the jump from each vertical profile directly by eye, comparing concentrations from approximately the top half of the ABL with the lowest ~100 m of the FT, assuming that the scale of turbulent entrainment is limited by the stability of the temperature inversion (Faloona et al., 2005). Errors in the jumps, estimated by the spread in the jumps and their approximate ambiguity, have been estimated to be ~10-100 % of the observed jumps (Tables 2 & 3). The scalar jump ($\Delta[C]_{(FT-ABL)}$), with C representing a generic scalar such as ozone, O_3, water vapor, q, or methane, CH_4, is usually negative for a compound with a surface source (e.g. water, methane, and ozone precursors), and a positive entrainment velocity holds for a turbulent boundary layer, which tends to grow at that rate in the absence of mean vertical wind (Eq. 1). Therefore, the sign of the entrainment flux is positive, upward, due to the entrainment dilution of FT air into the ABL – a downward flux of concentration deficit is equivalent to an upward flux.

In the absence of clouds and precipitation (in-situ sources or sinks) the water vapour budget equation is even simpler than that for ozone (Eq. 4):

$$\frac{\partial q}{\partial t} = -U\frac{\partial q}{\partial x} + \frac{(w'q')_s + w_e\,\Delta q_{FT-ABL}}{z_i} \qquad (6)$$

During our flights the first, second, and fourth terms above are measured by the aircraft allowing for the observation of the surface flux of water vapour. And in an exactly analogous manner we can use the aircraft measurements of methane to infer the surface flux, or average emission rate, of methane in the region. The surface latent heat flux, LH, divided by the latent heat of vaporization, L_v, $\frac{LH}{L_v} = (w'q')_s$, was taken from the NCEP/NARR dataset, and found to significantly underestimate our estimates in the regions of interest. We then look to the reference evapotranspiration (ET_o) at various sites throughout the Central Valley from the California Irrigation Management System (CIMIS). ET_o comes from standardized grass or alfalfa over which the measurement stations are situated, and it includes loss of water from the soil and plant surfaces. Although agriculture is prevalent in the area of interest it does not represent the entire land surface.

3 Discussion of Results

Below we discuss the various important results that can be extracted from a flight strategy targeting a fixed region of 50–100 km scale, and carefully tracking the changes in thermodynamic and chemical properties of the air mass. Because the sampling specifically targets the time of day when the boundary layer is actively entraining from the FT (excluding its initial phase of

Ian Faloona 9/18/2016 1:00 AM
Deleted: large …esoscale gradient in the C ... [10]
Ian Faloona [2] 9/12/2016 5:38 PM
Moved (insertion) [2] ... [11]
Ian Faloona [2] 9/12/2016 5:46 PM
Formatted ... [12]
Ian Faloona [2] 9/12/2016 5:46 PM
Deleted: is the deposition velocity represe ... [13]
Ian Faloona [2] 9/12/2016 5:50 PM
Formatted ... [14]
Ian Faloona [2] 9/12/2016 5:38 PM
Moved up [2]: , and P represents the net ... [15]
Ian Faloona [2] 9/12/2016 6:07 PM
Deleted: . ... [16]
Ian Faloona [2] 9/12/2016 6:10 PM
Formatted ... [17]
Justin 8/24/2016 12:18 PM
Comment [3]: I removed a few lines here ... [20]
Justin 8/24/2016 12:58 PM
Comment [4]: Also I tried to address in a ... [21]
Ian Faloona 9/18/2016 1:23 AM
Formatted ... [18]
Ian Faloona [2] 9/12/2016 6:10 PM
Deleted: is…diagnosed from vertical profi ... [19]
Ian Faloona [2] 9/12/2016 6:07 PM
Deleted: not seen encountered a rigorous. ... [22]
Ian Faloona 9/13/2016 6:29 PM
Deleted: 450-m,
Ian Faloona [2] 9/13/2016 10:56 AM
Deleted: ….Errors in observing the scalar ... [23]
Ian Faloona 9/18/2016 1:23 AM
Deleted: . ... [24]
Ian Faloona [2] 9/13/2016 10:57 AM
Formatted ... [25]
Ian Faloona 9/18/2016 1:04 AM
Formatted ... [26]
Ian Faloona [2] 9/13/2016 10:57 AM
Formatted ... [27]
Ian Faloona [2] 9/13/2016 11:00 AM
Deleted: defined this way …s positive, ... [28]
Ian Faloona 9/18/2016 1:12 AM
Deleted: Initially the water vapour budget ... [29]
Ian Faloona 9/13/2016 6:27 PM
Deleted: $\overline{(w'q')}_s\overline{(w'q')}_s$ +
Ian Faloona [2] 9/13/2016 11:44 AM
Deleted: $-w_e\,\Delta q\overline{(w'q')}_{FT-ABL}$ ... [30]
Ian Faloona 9/18/2016 1:34 AM
Deleted: .
Ian Faloona [2] 9/13/2016 11:46 AM
Deleted: The third term here is simply the ... [31]
Ian Faloona 9/13/2016 6:31 PM
Formatted ... [32]
Ian Faloona [2] 9/13/2016 11:51 AM
Formatted ... [33]
Ian Faloona 9/13/2016 6:28 PM
... [34]
Ian Faloona [2] 9/13/2016 11:47 AM
Deleted: Evapotranspiration is directly re ... [35]
Ian Faloona 9/18/2016 1:31 AM
Deleted: Using this value, ET_o, should ho ... [36]
Ian Faloona 9/18/2016 12:50 AM

'encroaching' through the residual layer), all of the results for entrainment rates, surface emissions of methane, evapotranspiration, and in situ photochemical production, all pertain to the period from 11:00 to 16:00 local standard time.

3.1 ABL Growth and Entrainment Rates

The airborne data measuring ABL growth rates are used to diagnose the entrainment rate by budgeting of z_i as expressed in Eq. (2). ABL heights and their diurnal changes are shown for all the flights in Fig. 4 compared with the corresponding RASS data presented in Bianco et al. (2011). The Chowchilla site is 50 km upwind from Fresno, and the Lost Hills site is just on the upwind edge of our sampling domain for the ArvinO3 study (Fig. 2). Both the boundary layer depths and their growth rates measured in the airborne experiments appear to be slightly lower than the Bianco et al. (2011) seasonal averages. The discrepancy is probably attributable to both airborne experiments specifically targeting the stagnation, high–pressure synoptic settings that characterize both the wintertime PM2.5 and summertime ozone episodes, which in principle suppress ABL development due to subsidence. Table 1 summarizes the estimated entrainment velocities from the two experiments, indicating a range between near zero (or below our detection limit of about 0.5 cm s^{-1}) to 2.4 cm s^{-1} during the wintertime in the central SJV (average of 1.5 ± 0.9 cm s^{-1}), and approximately 0.9 cm s^{-1} to 6.5 cm s^{-1} during the summertime over the southern SJV (average of 3.0 ± 2.1 cm s^{-1}.) Broadly comparable values have been observed in other continental studies: 4.3 cm s^{-1} during late July over grassland in the Netherlands in a study by de Arellano et al. (2004), 1.4 ± 0.3, 5.5 ± 1, and 9.6 ± 1.5 cm s^{-1} over the foothills of the Sierra Nevada adjacent to the California's Central Valley using isoprene flux measurements during June by Karl et al. (2013), and 5 ± 1 cm s^{-1} over the Ozark mountains in the southeastern U.S. during September by Wolfe et al. (2015). As far as we can tell, the data presented here are the first of their kind to estimate entrainment during the winter season, which although observed to be smaller as expected because of weaker surface heating, are critical to understanding the meteorological influence on the valley's PM2.5 episodes.

The entrainment velocities estimated in the two studies show evidence that they are linked to physically relevant surface parameters present during the flights. For example, the summertime entrainment velocities correlate well with the average ABL potential temperature (r^2 = 0.57, data not shown), insinuating that the forcing that heats the boundary layer (surface and consequent entrainment heat fluxes) is intimately linked to the entrainment rate. In a similar vein, the wintertime entrainment velocities correlate well with estimates of net surface radiation found in the NARR data set (r^2 = 0.68, data not shown.) A climatology of boundary layer heights reported by Pal & Haeffelin (2015) near Paris showed that although surface heat fluxes should most directly control the boundary layer height, a better correlation was found, on diurnal to seasonal time scales, with the surface down-welling shortwave radiation. While surface fluxes were not directly measured as part of the experimental set up, we turn to the surface solar radiation measured with pyranometers by the CIMIS network across the region. Figure 5 shows a very strong linear relationship with the surface pyranometer observations and the average boundary layer height for each flight. In fact, the linear fits for each separate experiment seem to be the same within the uncertainties of the fits, and the slopes of 1.5 m $(Wm^{-2})^{-1}$ are similar to those reported in Pal & Haeffelin (2015) of 1.7 m $(Wm^{-2})^{-1}$

Pal & Haeffelin (2015) further survey nearly a dozen past studies that reported ABL growth rates over different seasons ranging from 0.8 to 8.3 cm s^{-1}. There are two main reasons that these growth rates are not exactly comparable to the entrainment velocities reported here. First, most of these studies do not explicitly take into account horizontal or vertical z_i advection (the last two terms in Eq. (2)). Second, the convention used by many is to report ABL growth rates for the interval from when the surface heat flux reverses sign shortly after sunrise to the time when the boundary layer height is 90 % of its daily maximum. Such growth rates are thus a combination of the rapid growth through the nearly statically neutral residual layer in the morning and the

slower growth near midday when the ABL is actively entraining air from the free troposphere. For the chemical budgets under consideration in this work, we contend that it is more important to quantify the late morning to early afternoon entrainment mixing between the ABL and FT because entrainment of the residual layer in the early morning (sometimes called fumigation) represents merely a recycling of the previous day's boundary layer air (albeit from sources an overnight advection scale of order 100 km away). For the purposes of estimating regional source strengths or regional in situ photochemistry, we suggest that the more pertinent mixing process is the dilution of the anthropogenically influenced ABL air mass by the more global 'baseline' FT air, and we therefore exclude data from the morning period when the boundary layer is growing rapidly into the residual layer. Both of these differences lead to the realization that the ABL growth rates reported by Pal & Haeffelin (2015) and references therein, should be systematically larger than the entrainment velocities reported in this study, at least under fair weather conditions (subsidence). Our data from the DISCOVER–AQ wintertime study presented in Table 1 indicates that the advection and subsidence terms may not be first order, especially for longer period averages, and therefore may be comparable to other ABL growth rate statistics reported in the literature. This conjecture is consistent with conclusions from previous budget studies indicating that while advection may make a significant contribution to the scalar budget on any specific day, it may average out when considered on longer intervals (Conley et al., 2009; Faloona et al., 2010). A similar argument can be made for the vertical velocity term in Eq. (2); namely, that it may average to near zero across periods of instability and uplift, and periods of fair weather and subsidence. In a similar vein, the average z_i budgets for the southern SJV (ArvinO3 in Table 1) show a sizeable average orographic uplift and opposing horizontal advection of z_i, which together may be in a quasi-steady state nearly cancelling over long periods of weeks to months.

It follows that although not exactly equivalent to entrainment as described by Eq. (2), the range of ABL growth rates reported in the literature (from Pal & Haeffelin, 2015, and references therein) is nonetheless reasonably consistent with the data reported in Table 1. In the studies that report both winter and summer seasonal average ABL growth rates (Chen et al., 2001; van der Kamp & McKendry, 2010; Lewis et al., 2013; Schween et al., 2013; Korhonen et al., 2014; and Pal & Haeffelin, 2015) the summer to winter ratios tend to range from 1.4–3.0, with an average of 2.0. This is consistent with our results indicating entrainment rates 80 % higher in the SJV during summer than winter.

Bianco et al. (2011) postulate that convergence at the southern end of the SJV in summer leads to deeper ABLs there than in other parts of the valley, closer to the delta inflow region, which are influenced by strong marine layer inflow. A typical slope of ABL height up the SJV from Bianco et al. (2011) can be estimated from the Chowchilla and Lost Hills sites, which differ by about 750 m (from their Fig. 2) over a distance of approximately 175 km for the summer months. Applying to this gradient a calculated average along–valley wind at the top of the ABL of 2.5 m s^{-1} gives an advection term of -1.1 cm s^{-1}. This estimate compares well to the -1.15 cm s^{-1} reported in Table 1, derived from the NARR data set from our flight region 2 during summer. In addition, Bianco et al. (2011) make a rough estimate of convergence in the southern SJV by simply taking the difference in the horizontal along–valley wind at the two sites (2.5 m s^{-1} between Jun-Sep), divided by the distance between them, leading to ABL flow convergence of 1.4×10^{-5} s^{-1}. Such convergence would lead to an uplift of 1.4 cm s^{-1} at the top of a typical 1000 m boundary layer. This estimate is, again, right inline with our estimates from this study. From our findings it appears that the local time rate of change of observed ABL height nearly matches the entrainment rate when both are averaged over all the summer flights. The convergent uplift and the advection of ABL height appear to balance on average in the southern SJV. This suggests that the radio acoustic wind profiler data in the SJV, reported by Bianco et al. (2011), could be used to estimate entrainment rates by simply measuring the boundary layer growth during the midday.

Ian Faloona 9/19/2016 2:56 AM
Deleted: .

Ian Faloona 9/19/2016 2:56 AM
Deleted: E

Ian Faloona 9/13/2016 10:55 PM
Deleted: of

This idea is explored in Fig. 6, where we show the monthly average ABL growth rates observed year round by NOAA's wind profiler network operated across California's Central Valley during 2008 (Bianco et al., 2011). Additionally, the monthly average subsidence at boundary layer height is shown as captured in the NARR data set. Assuming that the advection term does not dominate at any of the sites in a long term average (other than at Lost Hills where it is possibly counterbalanced by the convergent uplift), we can get a sense of the general entrainment characteristics across the Central Valley throughout the year. For example, there appears to be stronger entrainment at lower latitudes in the valley (~3 cm s^{-1} annual peaks in the Sacramento vs. ~4 cm s^{-1} peaks in the San Joaquin Valley), possibly due to greater shortwave forcing or generally weaker stratification in the lower FT. It further seems that at most sites there is a definite peak in entrainment during the Spring but also a secondary maximum in the Autumn with a minimum during the mid–summer. This corresponds to the lowest ABL depths observed in the middle of summer as discussed by Bianco et al. (2011). In their analysis the authors suggest that the lower inversion heights of mid-summer are due to greater cold air advection through the delta and/or possibly the peak in irrigation in the heavily agriculturally controlled landscape of the Central Valley. Both effects serve to cool the ABL thereby increasing lower tropospheric stability (LTS) and suppressing entrainment. The lower right panel in Fig. 6 shows the LTS, as measured by the difference in potential temperatures between 750–900 hPa. The LTS minima in Spring and Autumn appear to coincide approximately with the peaks in entrainment more or less across the entire Central Valley.

3.2 Other Budget Residuals

Once the entrainment rate has been calculated for each flight it can be used to close the other scalar budget equations and calculate any single residual term, assuming all the others have been characterized. The time derivative and gradient terms were all calculated by applying a simple multi-linear regression on all flight data collected below the (time varying) ABL height as described in Conley et al. (2010).

3.2.1 Ozone Photochemical production

Figure 7 illustrates the distinction between ABL and FT air and the importance of entrainment mixing on an ozone exceedance day. The potential temperature and specific humidity on the left graph show the surface heating and nearly well–mixed ABL capped by the stable inversion with dry, warm air aloft. The right hand graph shows the enhanced NO_2 and O_3 within the ABL during the day because of the surface emissions of NO_x and the photochemical production of O_3 from those emissions in conjunction with reactive volatile organic compounds (RVOC). The ABL top, z_i, is indicated by the dashed line near 850 m. Given the jumps in O_3 and NO_2 evident at that height, and the estimated mean entrainment velocity for the entire flight, 5.1 cm s^{-1} (Table 1), the effect of entrainment dilution alone is causing a drop in surface O_3 and NO_2 concentrations by 4.0 and 0.32 ppb h^{-1}, respectively, demonstrating how important entrainment can be for understanding the temporal evolution of air pollutants measured near the surface. The consequences of horizontal advection can be seen in Fig. 8, which shows the spatial distribution of O_3 and NO_2 measured by the aircraft during the same day, 14 August 2013. The grey lines indicate the flight path over the course of the day, and because O_3 rises steadily throughout the flight, all the data is corrected to a common time (13:30 PST) by the observed mean temporal trend of 2.4 ppb h^{-1} and interpolated to a ~2 km gird across the domain. The spatial pattern shows a strong negative O_3 advection of -2.5 ppb h^{-1} into the Arvin area, but a countervailing positive NO_2 advection. Thus while consideration of the O_3 budget requires taking into account this inflow of lower O_3, the selfsame flow carries with it abundant precursors that boost the in-situ O_3 production near Arvin, the term that we infer through closure of the overall budget. This distribution of higher O_3 around Arvin was not observed on every day, but was more common on ozone exceedance days.

Ian Faloona 9/13/2016 9:41 PM
Deleted: B

Ian Faloona 9/13/2016 9:42 PM
Deleted: .

Because we only measured the NO_2 distribution once, it is more difficult to generalize, but the local maximum of NO_2 near Bakersfield has been reported elsewhere and is evident in seasonal satellite averages reported in Russell et al. (2010) and Pusede & Cohen (2012). The coloured circles in Fig. 8 are the 13:00-14:00 hourly average values from the CARB surface air quality network, and by and large confirm the large scale gradients observed by the aircraft.

In addition to applying our derived entrainment rates to close the O_3 budget (Eq. (4), results from which are presented in Table 2) we estimated the dry deposition term using a deposition velocity of 0.5 cm s^{-1}, with an estimated uncertainty of ± 0.25 cm s^{-1}, based on values reported in the literature for similar environments (Padro, 1996; Macpherson et al., 1995; Pio et al., 2000). The deposition term is the product of the deposition velocity and average ABL concentration divided by the ABL height. Dry deposition velocities are often reported with respect to a 10 m measurement, and although the lowest safe flight altitude is 150 m and we therefore do not have O_3 measurements at 10 m (aside from take offs and landings), the vertical gradients of O_3 tend to be no more than about 1 ppb per 100 m (Fig. 7), so we consider the uncertainty in the 10 m concentration to be ~ 2 ppb (3–4 % the mean O_3), and insignificant compared to the uncertainty in the deposition velocity of 50%. Ozone photochemical production (P) was estimated to be between 4.1 and 14.2 ppb h^{-1} in summer and 2.1–3.9 ppb h^{-1} in the winter. Comparisons between the winter and summer data sets are relevant. Although differences between the two sites could, in principle, arise due to varying local sources between Fresno and Bakersfield, the photochemical production is expected to be much lower in the winter with reduced actinic radiation fluxes. Note that there is a near tripling of the photochemical production between the two seasons, in winter the average is 2.8 ppb h^{-1} and in summer 8.2 ppb h^{-1}. O_3 production in the southern SJV, during the warm season, is believed to be NO_x-limited for most conditions except for weekdays (higher NO_x on average) when temperatures exceed 29° C, as proposed by Pusede et al. (2014), who investigated various factors in the production of ozone in the SJV. All of those conditions were met for the flights in the ArvinO3 study, and with the continued decrease in NO_x expected from the 7 year trend of -32% in Bakersfield reported by Russell et al. (2012) based on OMI satellite measurements of column NO_2, the conditions are only becoming more and more frequently NO_x–limited. A VOC:NO_x ratio proxy was derived from the airborne measurements of methane minus the global background methane from NOAA's Global Greenhouse Gas Reference Network (http://www.esrl.noaa.gov/gmd/ccgg/trends_ch4/) divided by the CARB surface air quality monitoring network NO_x concentrations measured during the flight hours. Although the VOC makeup of the SJV is fairly complex due to the preponderance of dairy farms and natural gas production, both of these source types are strong methane emitters (Gentner et al., 2014), so we consider observed methane to be a decent proxy for the overall abundance of non-methane VOCs. Figure 9 shows that the inferred O_3 production rates from both studies (Table 2) decrease with increasing VOC:NOx ratio proxy indicating that the SJV is mostly under NO_x–limited conditions.

Using a simplified box model constrained by observations of NO_x and OH reactivity, Pusede et al. (2014) estimate O_3 production rates ranging from 10–26 ppb h^{-1} at the Bakersfield CalNex supersite during May-June, 2010. This is approximately double the rates reported in this study using the budgeting technique, 4–14 ppb h^{-1} (Table 2), with an average uncertainty estimated to be ~1.3 ppb h^{-1}. The results reported by Pusede et al. (2014) are not net, but only the sum of the O_3 photochemical production channels. However, Pusede et al. (2014) estimate that the O_3 photochemical loss rates rarely exceed ~1.5 ppb h^{-1}, and we thus assume that this can only be a small part of the difference between our estimates and theirs. A much more significant difference is likely because of the fact that Pusede et al. (2014) use measurements made inside the metropolitan area of Bakersfield, while the flight data represents a region of about 4600 km^2 in which most of the land use is agricultural. Therefore, we expect the regional O_3 production to be smaller because it incorporates land outside of the urban centre where the NO_x is likely to be

Ian Faloona 9/19/2016 3:22 AM
Deleted: ,

Ian Faloona 9/19/2016 3:22 AM
Deleted: HO_x,

Ian Faloona 9/19/2016 3:22 AM
Deleted: VOC

Ian Faloona 9/19/2016 3:23 AM
Formatted: Superscript

considerably lower on average (Pusede & Cohen, 2012). Another estimate (Brune et al., 2016) from the same experiment reports midday ozone production rates of ~5 ppb h^{-1} from HO_2 alone, and assuming the organic peroxy radicals are nearly equivalent (as is often done, see Pusede et al., 2014 for example), then the total ozone production amounts to ~10 ppb h^{-1} in decent agreement with our measurements reported here. In a much earlier airborne attempt made at several sites across Europe and Asia, Lehning et al. (1998) estimate O_3 production in a similar way to ours but neglect temporal trends and dry deposition to come up with 2.5-3.5 ppb h^{-1}. Our estimates of those terms for the summer study sum to about 4 additional ppb h^{-1}, which would mean that their net photochemical production term could amount to 6.5-7.5 ppb h^{-1}, not far from our average of 8.1 ppb h^{-1}.

Baidar et al. (2013) performed a budget study based on a research flight conducted on June 15, 2010 in and around Bakersfield. Amongst the objectives of the study was the determination of an emission rate for NO_x and O_x (O_3 + NO_2) production rates from the urban area. They attempted a similar scalar budget approach using flight data obtained by remote sensing instruments (3 different lidar systems) aboard the NOAA Twin Otter, obtaining a range of O_3 production rates from 2.9–6.6 ppb h^{-1} with an area weighted average of 4.0 ppb h^{-1}. Within their volume of interest, they assumed the time rate of change of NO_x and O_x were zero, assuming that the horizontal flux divergence alone determines the source strength for their region. Aside from temporal changes (storage terms), they further neglected entrainment and dry deposition fluxes of these constituents. From their Fig. 5 indicating the diurnal signal of NO_x and O_x taken from the Bakersfield CARB monitoring station, we estimate a 2.2 ppb h^{-1} change in O_3 during their measurement time. In addition, they estimate a potential error of not including vertical mixing, or entrainment, to be less than 2%. Their estimate of the entrainment rate is on the low end of our range, at 1.2 cm s^{-1}, but when calculating their entrainment flux they use a delta O_x of about -4 ppb. Using our average observed jump across the ABL top of -13.4 ppb, an average entrainment velocity of 3.0 cm s^{-1}, and an average boundary layer height of 1000 m, along with a dry deposition velocity of 0.5 cm s^{-1}, the vertical terms give rise to a loss rate of approximately 2.6 ppb h^{-1}. This could easily explain the difference between their average of 4.0 ppb h^{-1} and our average of 8 ppb h^{-1}. But the comparison is imperfect because the ArvinO3 study specifically targeted ozone exceedance events (albeit only capturing 4 NAAQS and 6 California state exceedance days out of 11 flight days). During the day of the Baidar et al. (2013) study the O_3 peaked at only ~65 ppb based on the CARB surface monitoring network. Nevertheless, the comparison further points to the importance of treating all the budget terms in estimating net photochemical O_3 production. In our study the contribution to the O_3 budget from entrainment dilution is typically the same magnitude as the observed rise in O_3, and the latter alone only constitutes one-third of the total net production.

3.2.2 Methane Emission

For a scalar such as methane undergoing extremely slow chemistry (with a photochemical lifetime of about a decade), the budget equation can be easily solved for the surface emission rate:

$$F_s = \left(U\frac{\partial CH_4}{\partial x} + \frac{\partial CH_4}{\partial t}\right) z_i + F_{ent} \quad (7)$$

where the advection and temporal trend terms are observed directly by the aircraft, and F_{ent}, the entrainment flux, is estimated using the parameterization of Eq. 5 based on the observed jump in CH_4 across the ABL top and the entrainment velocity derived from the ABL height budget. Regional methane emissions from the DISCOVER–AQ campaign near Fresno were estimated to be 100 ± 100 Gg yr^{-1}, and from the Arvin-Bakersfield region they were estimated to be 170 ± 125 Gg yr^{-1} when averaged over each respective flight campaign. The second numbers reported above represent the estimated standard deviation of the mean value representing the spread in the measurements across the different days of each campaign, not the estimated error in the

Ian Faloona 9/20/2016 2:12 AM
Formatted: Superscript

Ian Faloona 9/20/2016 2:09 AM
Formatted: Subscript

Ian Faloona 9/20/2016 2:12 AM
Formatted: Superscript

Ian Faloona 9/20/2016 2:19 AM
Formatted: Subscript

Ian Faloona 9/20/2016 2:19 AM
Formatted: Superscript

Ian Faloona 9/20/2016 2:20 AM
Formatted: Superscript

Ian Faloona 9/20/2016 2:20 AM
Formatted: Superscript

Ian Faloona 9/20/2016 2:20 AM
Formatted: Superscript

Ian Faloona 9/18/2016 1:07 AM
Deleted: partaking in

Ian Faloona 9/19/2016 1:39 AM
Deleted: –

Justin 8/24/2016 3:57 PM
Deleted: +

Ian Faloona 9/19/2016 1:39 AM
Deleted:

measurements themselves. To obtain our in-situ emission estimate we multiplied our regionally averaged surface methane emission by the approximate horizontal area encompassed by the series of flights. For flight region one we estimated the horizontal area to be 9.5×10^8 m^2 because the flight pattern was simply across valley and the horizontal winds were light so there was little need to probe the direction of the mean advection. Flight region two covered a much larger area of 3.5×10^9 m^2 because the experiment specifically targeted a careful mapping of the up-valley advection term in the O_3 budget. In a recent work by Kort et al. (2014) using the Scanning Imaging Absorption Spectrometer for Atmospheric Chartography (SCIAMACHY) instrument from 2003–2009 the column-averaged CH_4 mole fractions over the U.S. are used to estimate surface emissions. Although the thrust of that study was the 'hot spot' observed over the four corners region of New Mexico, it is interesting to note that the second largest spot (their Fig. 1) that emerges in the satellite climatology is located in the southern San Joaquin Valley of California. Using the California Greenhouse Gas Emission Measurement (CALGEM; http://calgem.lbl.gov/prior_emission.html) inventory we estimated the emissions from each sector for both flight regions. The emission estimates have been scaled to the 2013 total CH_4 emission estimate for California of 41.1 TgCO2eq provided by CARB. Inventory emissions from flight region one was found to be a total of 27.7 Gg yr^{-1} and from region two 71.1 Gg yr^{-1}. Comparing these to the in-situ estimates of this study we find our estimates to be 3.6 and 2.4 times greater than the scaled CALGEM inventory estimates, respectively. According to the breakdown in sources found in the CALGEM database we estimated the fractional coverage of each source type for the two experiments. The first region sampled in winter near Fresno for the DISCOVER–AQ project was found to bear 54% fossil fuel related sources, with the majority of the balance coming from dairies (25%) and other livestock (9%) and landfills (11%). Flight region two flown during the summertime around Bakersfield was more dominated by dairies (73%), with most of the rest fossil related (17%). The difference in make-up of the two regions is broadly consistent with the finding expounded by Miller et al. (2013) that ruminant sources of methane appear to be approximately twice as large as current inventories hold, while fossil fuel sources are nearly six times larger than the present inventories indicate. This could account for the greater discrepancy found in the DISCOVER–AQ data where observed emissions are more heavily influenced by sources associated with fossil fuels.

To further examine the observed variability of the methane emissions in the southern SJV, where the sources are predominantly from dairies and thus derive from enteric and manure methanogenesis, the temperature dependence is presented in Fig. 10 in an Arrhenius type plot. In general, the temperature response of microbial activity (ultimately the source of methane emission associated with livestock) is often quantified by an Arrhenius equation: i.e., $\text{rate} = A \bullet \exp(-Ea/RT)$, where A is a pre-exponential factor, E_a is the activation energy, R is the universal gas constant (8.314 J mol^{-1} K^{-1}), and T is the absolute temperature. Figure 10 shows the natural log of our estimates of methane emissions, at temperatures below the optimum (peak methane production occurs in the mesophillic range of 30–37°C). The results of Elsgaard et al. (2016) indicate a peak in methane production near 38°C in cattle slurries. In order to compare most appropriately, we removed the CH_4 emission rate estimate of the flight of 9 June 2014 when the air temperatures exceeded 39°C, and we set the emission estimate to 0 (from -20 Gg yr^{-1}, within the method's uncertainty) for the 30 September flight, which was the coldest day of the experiment (afternoon average surface temperature in Bakersfield of 25.7°C). The resultant data in Fig. 10 shows signs of an Arrhenius type behaviour in the dominant methane sources in the southern end of the SJV, and moreover the activation energy, E_a, derived from the fit is 76 kJ mol^{-1} is very similar to that found by Elsgaard et al. (2016) of 81 kJ mol^{-1}. The correlation coefficient for the linear fits does not change significantly when the flight data from the two dates mentioned above are included (r^2 of 0.54 instead of 0.58).

3.2.3 Surface Latent Heat Flux

Rearrangement of the water budget relationship Eq. (6), in a fashion similar to that of methane, leads to the ready estimation of surface latent heat fluxes for each campaign. The average for summer flights around Bakersfield was 284 W m^{-2} and for winter outside of Fresno it was 90 W m^{-2}. Comparing these values to reference evapotranspiration estimated by the CIMIS network (515 and 160 W m^{-2}, respectively) we find that both experiments predict virtually identical fractions, 55%, occurring across the regions. This is likely the result of mixed land uses dominated by agriculture with interspersed fallow and actively growing plots. As expected the latent heat fluxes were observed to be lower in winter as the solar radiation is smaller and crop demand for water is reduced, but in both seasons it was found to be dramatically larger than the surface latent heat fluxes used in the NARR reanalysis data. This result, which most likely arises due to the lack of accurate irrigation information in the NARR land surface model, is significant because it is most likely the reason why the reanalysis data reports boundary layers that are very much higher than observed, therefore this data should be used with caution by the community.

4 Error Analysis

The estimated errors from each term in each budget equation are reported in Tables 1-3. All of the airborne data collected within the (time dependent) ABL is used to calculate temporal trends and horizontal gradient terms using a multiple linear regression. Each term's standard error was estimated from a residual taken as the difference between the predicted values from the regression and the actual values normalized by the number of data points. Omega values taken from NARR reanalysis were assumed to have an error of ± 0.05 Pa s^{-1} (~ 0.5 cm s^{-1}), which we took to be a fairly conservative estimate. Albrecht et al. (2016) utilized vertical velocity from ECMWF reanalysis data, originally as omega values, in the same inversion height budget (Equation 2) and they equally arbitrarily estimate the error as ± 0.1 cm s^{-1}, a factor of five smaller than ours. The errors are propagated through the budget equations, and in the case of Eq. 2 all the coefficients are unity so the variances simply add together. The overall uncertainties in the entrainment velocities average to about 1 cm/s, which come from nearly equal parts uncertainty in the temporal trend, advection, and the reanalysis vertical velocities. We note that such uncertainty magnitudes are not uncommon for such a difficult, yet important, parameter to measure (de Arellano et al. 2004; de Roode & Duynkerke, 1997; Bretherton et al, 1995; Wolfe et al., 2015.) For the ozone budget we estimate the errors in the O_3 jump between ABL and FT by eye and these range from ~10-100% of the jump values. This is combined with the entrainment velocity error from each flight to derive the combined uncertainty of the entrainment flux. For the deposition velocity we estimate an uncertainty of about 0.25 cm/s based on a range of midday values reported in the literature for similar environments. We do not include uncertainty in the boundary layer height because we expect it to be relatively small at ~5% (~50 m of ~1000 m.) The resultant relative errors in the net ozone production amounts to only ~15-40%. It is difficult to discern exact uncertainties from other studies to compare. Pusede et al. (2014) do not make any mention of uncertainty in their reports of this rate, while Brune et al. (2016) show that their estimated ozone production rates are twice as large when using observed HO_2 than with modeled values. Errors were taken from instrumental specifications when considering the error in mean quantities like ozone or methane concentration, and mean wind (for the advection terms). The errors in our methane emissions estimates are comparable to the estimates themselves, primarily because the leading term that balances the surface emissions is the entrainment dilution. Nevertheless, we feel that over the course of many flights the mission averages take on greater significance (although we do not divide it by the square root of the number of flights.) Moreover, because the flight to flight variations appear to exhibit an Arrhenius dependence on temperature, we believe that the methane emissions reported here are meaningful.

Ian Faloona 9/13/2016 10:24 PM
Deleted: indicates

Ian Faloona 9/13/2016 10:25 PM
Deleted: has

Ian Faloona 9/20/2016 12:45 AM
Deleted: from the scalar budgets were calculated

Ian Faloona 9/20/2016 12:47 AM
Deleted: and

Ian Faloona 9/20/2016 12:46 AM
Deleted: the

Ian Faloona 9/20/2016 12:46 AM
Deleted: in them

Ian Faloona 9/20/2016 12:47 AM
Deleted: taken

Ian Faloona 9/20/2016 12:48 AM
Deleted: as a standard error of the estimate

Ian Faloona 9/20/2016 12:48 AM
Deleted: The standard error of the estimat ... [37]

Ian Faloona 9/20/2016 12:51 AM
Deleted: be

Ian Faloona 9/20/2016 12:52 AM
Deleted: of the error

Ian Faloona 9/20/2016 12:53 AM
Deleted: as well

Ian Faloona 9/20/2016 12:54 AM
Deleted: e

Ian Faloona 9/20/2016 12:54 AM
Deleted: d

Ian Faloona 9/20/2016 12:54 AM
Deleted: that

Ian Faloona 9/20/2016 12:57 AM
Deleted: of the average was about

Ian Faloona 9/20/2016 12:55 AM
Formatted ... [38]

Ian Faloona 9/20/2016 1:07 AM
Deleted: In addition, they concluded that t ... [39]

Ian Faloona 9/20/2016 1:33 AM
Formatted ... [40]

Ian Faloona 9/20/2016 1:47 AM
Formatted ... [41]

Ian Faloona 9/20/2016 1:30 AM
Deleted: Other

Ian Faloona 9/20/2016 1:52 AM
Deleted: e

Ian Faloona 9/20/2016 1:52 AM
Deleted: also estimated, including; the sca ... [42]

Ian Faloona 9/20/2016 1:55 AM
Deleted: regional

Ian Faloona 9/20/2016 1:53 AM
Deleted: , etc

Ian Faloona 9/20/2016 1:54 AM
Deleted: . Each variable from our compou ... [43]

5 Conclusions

In situ measurement via targeted aircraft campaigns can help us understand key factors in boundary layer dynamics, including entrainment. It is propitious when it comes to probing complex mesoscale features, i.e. areas influenced by mountain–valley dynamics. A better understanding of entrainment is integral to understanding air quality on the ground, and it has potential applications in quantifying the significance of trans–boundary contributions to local air pollution. The simple, yet novel scalar budgeting technique based on focused airborne sampling of the ABL outlined here is invaluable to boundary layer studies and can help inform atmospheric chemistry studies. From our analysis of the inversion height budget, the boundary layer height advection balances the mean upward vertical wind forced by orographic convergence at the southern end of the SJV. This balance permits the measurement of entrainment by simply measuring the change in ABL height throughout the daytime. The NOAA RASS sounders would suffice in this region to make regular measurements of entrainment, and analysis of data reported by Bianco et al. (2011) from 2008 shows bimodal peaks in entrainment in early spring (March) and late summer (August) at Lost Hills approximately 40 km northwest of Bakersfield (between the two target regions of this study.) Similar bimodal peaks in entrainment were found during spring and autumn for sites throughout California's Central Valley, and may be due to the minima LTS in those transition seasons.

Subsidence in complex topography is not very well understood, cannot be measured accurately, and is likely to be quite sizeable. Future studies should target a better understanding of the large scale vertical velocities in the lower atmosphere to better elucidate the mixing and transport. One way this might be achieved is to deploy an airborne investigation to measure the surface heat fluxes and inversion strength and observe the growth rate and horizontal gradients of the valley boundary layers. By using equation (2) the subsidence rate could be measured indirectly given that the advection and time rate of change terms were observed directly, and using a simple mixed layer dynamical model (e.g. CLASS: http://classmodel.github.io/) to estimate the entrainment rate.

Applying the entrainment results of the budgeting of ABL height to the other scalars then leads to significant insights into their sources and controlling variables. It was found that entrainment dilution and dry deposition of O_3 are comparable in magnitude (but opposite in sign) to the observed time rate of change, which itself is only one-third of the net photochemical production during the O_3 season in the Bakersfield/Arvin area. While advection of O_3 into the town of Arvin is consistently observed to be negative (lower O_3 air being brought in by the up–valley flow), a steady advection of high NO_x upstream seems to keep the in situ production elevated in the Arvin area. Moreover, a proxy for VOC to NO_x ratio was used from the airborne methane and the surface air quality network NO_x to show that O_3 production is NO_x–limited in the southern SJV in summer and mid–SJV in the winter. The methane budgets revealed stronger sources in the SJV than those in the CALGEM database, with a greater disparity in the wintertime near Fresno, where there is a greater fraction of methane from petroleum related sources. And finally the water vapour budget showed that the evapotranspiration in these regions are approximately 55% of their reference values (with respect to well watered and groomed grass) according to the CIMIS network in both seasons. These evapotranspiration rates are much larger than contained in the NARR data set, which does not appear to include realistic irrigation in its land surface module, and this will be a source of significant overestimation of boundary layer heights throughout the year in the Central Valley.

This study shows that aircraft-based ABL budgeting studies can help to constrain regional emission rates and photochemical production rates – both of which are poorly constrained in current models. Emission rates derived by these methods bypass a lot of the complex issues associated with inverse modelling because the scales are smaller (covering areas of 30-50 km linear scale),

Ian Faloona [2] 9/9/2016 6:07 PM
Deleted: , and it is easy to apply with sufficient probing of the ABL for any given region.

Ian Faloona 9/19/2016 1:36 AM
Deleted:

and do not rely on highly parameterized vertical mixing processes. Moreover, by measuring the specific terms in the ozone budget, detailed comparisons with photochemical models can uncover distinct weaknesses in our current models and discern whether the difficulties lie in dynamical (transport) or chemical aspects of the numerical efforts.

Acknowledgements

The ArvinO3 study was made possible by backing from the San Joaquin Valley Air Pollution Control District. We would especially like to thank David Lighthall, may he rest in peace, for his enthusiastic support, many fruitful discussions, and for his friendship. Flight time to participate in NASA's DISCOVER-AQ was provided by the Bay Area Air Quality Management District, and we thank the former's Jim Crawford and the latter's Saffet Tanrikulu for making it happen. We are very indebted to Irina Djalalova, Laura Bianco, and James Wilczak for providing us with their RASS boundary layer height data from across the Central Valley. We further thank Doug Baer and his colleagues at Los Gatos Research for the generous loan of their NO_2 spectrometer, and Marc Fischer for freely sharing his CALGEM methane source inventory. The reviews by three anonymous referees helped to improve the clarity of the manuscript, and we thank them for their efforts.

References

Albrecht, B., Fang, M., Ghate, V.: Exploring Stratocumulus Cloud-Top Entrainment Processes and Parameterizations by Using Doppler Cloud Radar Observations, J. Atmos. Sci. 73(2), 729-42, 2016.

Al-Saadi, J., Soja, A., Pierce, R. B., Szykman, J., Wiedinmyer, C., Emmons, L., Kondragunta, S., Zhang, X. Y., Kittaka, C., Schaack, T., and Bowman, K.: Intercomparison of near-real-time biomass burning emissions estimates constrained by satellite fire data, J. Appl. Remote Sens., 2, 24, 2008.

Angevine, W. M.: Errors in mean vertical velocities measured by boundary layer wind profilers, J Atmos Ocean Tech, 14, 565-569, Doi 10.1175/1520-0426(1997)014<0565:Eimvvm>2.0.Co;2, 1997.

Baidar, S.: Combining Active and Passive Airborne Remote Sensing to Quantify NO2 and Ox Production near Bakersfield, CA, BJECC British Journal of Environment and Climate Change 3(4), 2013.

Ball, F.K., Control of Inversion Height by Surface Heating, Quart. J. Roy. Meteo. Soc., 482-494, 1960.

Bandy, A., Faloona, I. C., Blomquist, B. W., Huebert, B. J., Clarke, A. D., Howell, S. G., Mauldin, R. L., Cantrell, C. A., Hudson, J. G., Heikes, B. G., Merrill, J. T., Wang, Y., O'Sullivan, D. W., Nadler, W. and Davis, D. D.: Pacific Atmospheric Sulfur Experiment (PASE): Dynamics and Chemistry of the South Pacific Tropical Trade Wind Regime, J. Atmos. Chem., 68(1), 5-25, 2011.

Bao, J. W., Michelson, S. A., Persson, P. O. G., Djalalova, I. V., and Wilczak, J. M.: Observed and WRF-simulated low-level winds in a high-ozone episode during the Central California Ozone Study, J. Appl. Meteorol. Climatol., 47, 2372-2394, 10.1175/2008jamc1822.1, 2008.

Bianco, L., Djalalova, I. V., King, C. W. and Wilczak, J. M.: Diurnal Evolution and Annual Variability of Boundary-Layer Height and Its Correlation to Other Meteorological Variables in California's Central Valley, Bound.-Lay. Meteorol., 140, 491-511, 2011.

Brandt, A. R., Heath, G. A., Kort ,E. A., O'sullivan, F., Petron, G., Jordaan, S. M., Tans, P., Wilcox, J., Gopstein, A. M., Arent, D., Wofsy, S., Brown, N. J., Bradley, R., Stucky, G. D., Eardley, D. and Eardley, R.: Methane Leaks from North American Natural Gas Systems, Science, 343, 733-35, 2014

Chen, W. B., Kuze, H., Uchiyama, A., Suzuki, Y., and Takeuchi, N.: One-year observation of urban mixed layer characteristics at Tsukuba, Japan using a micro pulse lidar, Atmos. Environ., 35, 4273-4280, 10.1016/s1352-2310(01)00181-9, 2001.

Conley, S. A., Faloona, I. C., G. Miller, H., Lenschow, D. H., Blomquist, B. and Bandy, A.: Closing the Dimethyl Sulfide Budget in the Tropical Marine Boundary Layer during the Pacific Atmospheric Sulfur Experiment, Atmos. Chem. Phys., 9, 8745-756, 2009.

Conley, Stephen A., Faloona, I. C., Lenschow, D. H., Campos, T., Heizer, C., Weinheimer, A., Cantrell, C. A., Mauldin, R. L., Hornbrook, R. S., Pollack, I. and Bandy, A.: A Complete Dynamical Ozone Budget Measured in the Tropical Marine Boundary Layer during PASE, J. Atmos. Chem., 68, 55-70, 2011.

Conley, S. A., Faloona, I. C., Lenschow, D. H., Karion, A. and Sweeney, C.: A Low-Cost System for Measuring Horizontal Winds from Single-Engine Aircraft, J. Atmos. Ocean. Technol., 31(6), 1312-320, 2014.

deArellano, Vilà-Guerau, J., Gioli, B., Miglietta, F., Jonker, H. J. J., Baltink, H. K., Hutjes, R. W. A. and Holtslag, A. A. M.: Entrainment Process of Carbon Dioxide in the Atmospheric Boundary Layer, J. Geophys. Res. 109(D18), 2004.

Elsgaard, L., Olsen, A. B., and Petersen, S. O.: Temperature response of methane production in liquid manures and co-digestates, Sci Total Environ, 539, 78-84, 10.1016/j.scitotenv.2015.07.145, 2016.

Faloona, I. C., Lenschow, D. H., Campos, T., Stevens, B., Van Zanten, M., Blomquist, B., Thornton, D., Bandy, A. and Gerber, H.: Observations of Entrainment in Eastern Pacific Marine Stratocumulus Using Three Conserved Scalars, J. Atmos. Sci. 62(9), 3268-285, 2005.

Faloona, I., Conley, S. A., Blomquist, B., Clarke, A. D., Kapustin, V., Howell, S., Lenschow, D. H. and Bandy A. R.: Sulfur Dioxide in the Tropical Marine Boundary Layer: Dry Deposition and Heterogeneous Oxidation Observed during the Pacific Atmospheric Sulfur Experiment, J. Atmos. Chem. 63(1), 13-32, 2010.

Frenzel, C.W.:Diurnal wind variations in central California, J. Appl. Meteorol., 1, 405–412, 1962.

Gentner, D. R., Ford, T. B., Guha, A., Boulanger, K., Brioude, J., Angevine, W. M., de Gouw, J. A., Warneke, C., Gilman, J. B., Ryerson, T. B., Peischl, J., Meinardi, S., Blake, D. R., Atlas, E., Lonneman, W. A., Kleindienst, T. E., Beaver, M. R., St Clair, J. M., Wennberg, P. O., VandenBoer, T. C., Markovic, M. Z., Murphy, J. G., Harley, R. A., and Goldstein, A. H.: Emissions of organic carbon and methane from petroleum and dairy operations in California's San Joaquin Valley, Atmospheric Chemistry and Physics, 14, 4955-4978, 10.5194/acp-14-4955-2014, 2014.

Hays, T.P., Kinney, J. K., Wheeler, N. J.: California surface wind climatology. California Air Resources Board Rep., Sacramento, 1984.

Karl, T., Misztal, P. K., Jonsson, H. H., Shertz, S., Goldstein, A. H. and Guenther, A. B.: Airborne Flux Measurements of BVOCs above Californian Oak Forests: Experimental Investigation of Surface and Entrainment Fluxes, OH Densities, and Damköhler Numbers, J. Atmos. Sci., 70(10), 3277-287, 2013.

Kawa, S. R. and Pearson Jr., R.: An observational study of stratocumulus entrainment and thermodynamics. J. Atmos. Sci., 46, 2649–2661, 1989a.

——, and ——.: Ozone budgets from the dynamics and chemistry of marine stratocumulus experiment, J. Geophys. Res., 94, 9809–9817, 1989b.

Korhonen, K., Giannakaki, E., Mielonen, T., Pfuller, A., Laakso, L., Vakkari, V., Baars, H., Engelmann, R., Beukes, P., Van Zyl, P. G., Ramandh, A., Ntsangwane, L., Josipovic, M., Tiitta, P., Fourie, G., Ngwana, I., Chiloane, K., and Komppula, M.: Atmospheric boundary layer top height in South Africa: measurements with lidar and radiosonde compared to three atmospheric models, Atmos. Chem. Phys., 14, 4263-4278, 10.5194/acp-14-4263-2014, 2014.

Kort, E. A., Frankenberg, C., Costigan, K. R., Lindenmaier, R., Dubey, M. K. and Wunch, D.: Four Corners: The Largest US Methane Anomaly Viewed from Space, Geophys. Res. Lett., 41(19), 6898-903, 2014.

Lenschow, D. H.: Airplane measurements of planetary boundary layer structure, J. Appl. Meteorol., 9, 874-884, 1970.

Lenschow, D. H., Pearson, R. and Stankov, B. B.: Estimating the Ozone Budget in the Boundary Layer by Use of Aircraft Measurements of Ozone Eddy Flux and Mean Concentration, J. Geophys. Res., 86(C8), 7291, 1981.

Lenschow, D. H., Paluch, I. R., Bandy, A. R., Thornton, D. C., Blake, D. R., and Simpson, I.: Use of a mixed-layer model to estimate dimethylsulfide flux and application to other trace gas fluxes, J Geophys Res-Atmos, 104, 16275-16295, Doi 10.1029/1998jd100090, 1999.

Lenschow, D. H., Savic-Jovcic, V., and Stevens, B.: Divergence and vorticity from aircraft air motion measurements, J Atmos Ocean Tech, 24, 2062-2072, 10.1175/2007JTECHA940.1, 2007.

Lewis, J. R., Welton, E. J., Molod, A. M., and Joseph, E.: Improved boundary layer depth retrievals from MPLNET, J. Geophys. Res.-Atmos., 118, 9870-9879, 10.1002/jgrd.50570, 2013.

Li, Y. P., Smith, R. B., and Grubisic, V.: Using Surface Pressure Variations to Categorize Diurnal Valley Circulations: Experiments in Owens Valley, Monthly Weather Review, 137, 1753-1769, 10.1175/2008mwr2495.1, 2009.

Lin, Y. L., and Jao, I. C.: A Numerical Study Of Flow Circulations In The Central Valley Of California And Formation Mechanisms Of The Fresno Eddy, Monthly Weather Review, 123, 3227-3239, 1995.

Macpherson, J. I., Desjardins, R. L., Schuepp, P. H., and Pearson, R.: Aircraft-Measured Ozone Deposition In The San-Joaquin Valley Of California, Atmospheric Environment, 29, 3133-3145, 1995.

Miller, S. M., Wofsy, S. C., Michalak, A. M., Kort, E. A., Andrews, A. E., Biraud, S. C., Dlugokencky, E. J., Eluszkiewicz, J., Fischer, M. L., Janssens-Maenhout, G., Miller, B. R., Miller, J. B., Montzka, S. A., Nehrkorn, T., and Sweeney, C.: Anthropogenic emissions of methane in the United States, Proceedings of the National Academy of Sciences of the United States of America, 110, 20018-20022, 10.1073/pnas.1314392110, 2013.

Moore, G. E., Daly, C., Liu, M. K., and Huang, S. J.: Modeling Of Mountain-Valley Wind Fields In The Southern San-Joaquin Valley, California, Journal of Climate and Applied Meteorology, 26, 1230-1242,1987.

Nichols, S.: The dynamics of stratocumulus: Aircraft observations and comparisons with a mixed layer model, Quart. J. Roy. Meteor. Soc., 110, 783–820, 1984.

Ozone 8-hour plan 2007 Executive Summary, www.valleyair.org/Air_Quality_Plans/docs/AQ_Ozone_2007_Adopted/03%20Executive%20Summary.pdf, 2007.

Padro, J.: Summary of ozone dry deposition velocity measurements and model estimates over vineyard, cotton, grass and deciduous forest in summer, Atmospheric Environment, 30, 2363-2369, 10.1016/1352-2310(95)00352-5, 1996.

Pal, S., and Haeffelin, M.: Forcing mechanisms governing diurnal, seasonal, and interannual variability in the boundary layer depths: Five years of continuous lidar observations over a suburban site near Paris, J Geophys Res-Atmos, 120, 10.1002/2015JD023268, 2015.

Pio, C. A., Feliciano, M. S., Vermeulen, A. T., and Sousa, E. C.: Seasonal variability of ozone dry deposition under southern European climate conditions, in Portugal, Atmos Environ, 34, 195-205, Doi 10.1016/S1352-2310(99)00276-9, 2000.

Pusede, S. E., and Cohen, R. C.: On the observed response of ozone to NOx and VOC reactivity reductions in San Joaquin Valley California 1995-present, Atmospheric Chemistry and Physics, 12, 8323-8339, 10.5194/acp-12-8323-2012, 2012.

Pusede, S. E., Gentner, D. R., WooldridgeP. J., Browne, E. C., Rollins, A. W., Min, K. E., Russell, A. R., Thomas, J., Zhang, L., Brune, W. H., Henry, S. B., Digangi, J. P., Keutsch, F. N., Harrold, S. A., Thornton, J. A., Beaver, M. R., St. Clair, J. M., Wennberg, P. O., Sanders, J., Ren, X., Vandenboer, T. C., Markovic, M. Z., Guha, A., Weber, R., Goldstein, A. H. and Cohen, R. C.: On the Temperature Dependence of Organic Reactivity, Nitrogen Oxides, Ozone Production, and the Impact of Emission Controls in San Joaquin Valley, California, Atmos. Chem. Phys. 14(7), 3373-395, 2014.

Rampanelli, G., Zardi, D., and Rotunno, R.: Mechanisms of up-valley winds, J. Atmos. Sci., 61, 3097-3111, 10.1175/jas-3354.1, 2004.

Russell, A. R., Valin, L. C., Bucsela, E. J., Wenig, M. O., and Cohen, R. C.: Space-based Constraints on Spatial and Temporal Patterns of NOx Emissions in California, 2005-2008, Environ. Sci. Technol., 44, 3608-3615, 10.1021/es903451j, 2010.

Schmidl, J., and Rotunno, R.: Mechanisms of Along-Valley Winds and Heat Exchange over Mountainous Terrain, J. Atmos. Sci., 67, 3033-3047, 10.1175/2010jas3473.1, 2010.

Schultz, H.B., Akesson, N.B., Yates, W.E.: The delayed ‘sea breezes’ in the Sacramento Valley and the resulting favorable conditions for application of pesticides, Bull. Am. Meteorol. Soc. 42, 679–687, 1961.

Schween, J. H., Hirsikko, A., Lohnert, U., and Crewell, S.: Mixing-layer height retrieval with ceilometer and Doppler lidar: from case studies to long-term assessment, Atmos. Meas. Tech., 7, 3685-3704, 10.5194/amt-7-3685-2014, 2014.

Tennekes, H., A Model for the Dynamics of the Inversion Above a Convective Boundary Layer, J. Atmos. Sci., 30, 558-567, 1973.

van der Kamp, D., and McKendry, I.: Diurnal and Seasonal Trends in Convective Mixed-Layer Heights Estimated from Two Years of Continuous Ceilometer Observations in Vancouver, BC, Bound-Lay Meteorol, 137, 459-475, 10.1007/s10546-010-9535-7, 2010.

Warner, J. and Telford J. W.: A check of aircraft measurements of vertical heat flow, J. Atmos. Sci., 22, 463-465, 1965.

Whiteman, C. D.: Observations of thermally developed wind systems in mountainous terrain. Chapter 2 in: Atmospheric Processes over Complex Terrain, edited by: Blumen, W., Meteor. Mon., 23, 5–42, Published by Amer. Meteor. Soc., Boston, MA, 1990.

Wolfe, G. M., Hanisco, T. F., Arkinson, H. L., Bui, T. P., Crounse, J. D., Dean-Day, J., Goldstein, A., Guenther, A., Hall, S. R., Huey, G., Jacob, D. J., Karl T., Kim, P. S., Liu, X., Marvin, M. R., Mikoviny, T., Misztal, P. K., Nguyen, T. B., Peischl, J., Pollack, I., Ryerson, T., St. Clair, J. M., Teng, A., Travis, K. R., Ullmann, K., Wennberg, P. O. and Wisthaler, A.: Quantifying

Sources and Sinks of Reactive Gases in the Lower Atmosphere Using Airborne Flux Observations, Geophys. Res. Lett., 42(19), 8231-240, 2015.

Wood, R., and Bretherton, C. S.: Boundary layer depth, entrainment, and decoupling in the cloud-capped subtropical and tropical marine boundary layer, J. Clim., 17, 3576-3588, 2004.

Zaremba, L. L., and Carroll, J. J.: Summer wind flow regimes over the Sacramento Valley, Journal of Applied Meteorology, 38, 1463-1473, 1999.

Zhong, S., Whiteman, C. D. and Bian, X.: Diurnal Evolution of Three-Dimensional Wind and Temperature Structure in California's Central Valley, J. Appl. Meteor. 43(11), 1679-699, 2004.

	dzi/dt (cm s^{-1})	Sfc-P Tend (cm s^{-1})	Omega (cm s^{-1})	W (cm s^{-1})	z_i advection (cm s^{-1})	w_e (cm s^{-1})
1/16/13	1.13(0.29)	-0.16 (0.01)	0.8(0.5)	-1.0(0.5)	0.08(0.12)	2.08(0.59)
1/18/13	1.14(0.60)	-0.16(0.01)	0.4(0.5)	-0.6(0.5)	0.05(0.42)	1.69(0.89)
1/20/13	0.56(0.63)	-0.16(0.01)	0.8(0.5)	-1.0(0.5)	0.04(0.20)	1.56(0.83)
1/21/13	0.72(0.22)	-0.11(0.01)	-0.9(0.5)	0.9(0.5)	0.07(0.06)	-0.21(0.55)
1/22/13	1.85(0.49)	-0.16(0.01)	-0.1(0.5)	1.1(0.5)	-0.21(0.95)	0.96(1.18)
1/30/13	3.57(0.58)	-0.05(0.01)	-1.7(0.5)	1.6(0.5)	-0.44(0.14)	2.39(0.77)
2/4/13	1.38(0.60)	-0.21(0.01)	0.5(0.5)	-0.8(0.5)	0.06(0.10)	2.13(0.80)
Averages	1.48(0.49)	-0.14(0.01)	-0.0(0.5)	-0.0(0.5)	-0.05(0.14)	1.51(0.80)
Std Dev of avg	1.01	0	0.11	1.14	0.2	0.89
6/26/13	1.23(0.39)	-0.12(0.01)	0.3(0.5)	-0.4(0.5)	0.75(1.20)	0.86(1.36)
6/27/13	3.79(0.72)	-0.12(0.01)	-2.7(0.5)	2.5(0.5)	-0.20(1.32)	1.51(1.59)
6/28/13	4.28(1.17)	-0.18(0.01)	-1.5(0.5)	1.3(0.5)	-1.67(3.28)	4.69(3.52)
8/13/13	4.11(0.35)	-0.17(0.01)	-0.8(0.5)	0.6(0.5)	-1.47(1.50)	4.98(1.62)
8/14/13	2.42(0.79)	-0.12(0.01)	-1.7(0.5)	1.5(0.5)	-4.24(2.64)	5.14(2.80)
8/15/13	2.54(0.75)	-0.11(0.01)	-2.6(0.5)	2.5(0.5)	-1.03(0.70)	1.10(1.14)
9/28/13	1.20(0.02)	-0.17(0.01)	0.1(0.5)	-0.3(0.5)	0.00(0.02)	1.45(0.50)
9/29/13	2.75(0.47)	-0.17(0.01)	-1.9(0.5)	1.7(0.5)	-0.02(0.10)	1.05(0.69)
9/30/13	2.95(0.46)	-0.17(0.01)	-1.1(0.5)	0.9(0.5)	0.81(2.51)	1.23(2.60)
6/8/14	4.95(0.85)	-0.12(0.01)	-1.4(0.5)	1.2(0.5)	-0.70(0.34)	4.41(1.05)
6/9/14	2.83(1.00)	-0.21(0.01)	-1.5(0.5)	1.2(0.5)	-4.84(5.84)	6.52(5.95)
Averages	3.00(0.63)	0.15(0.01)	1.3(0.5)	1.2(0.5)	2.30(1.77)	2.99(2.07)
Std Dev of avg	1.2	0.01	0.1	0.93	1.86	2.13

Table 1: Entrainment rate table for both studies (DISCOVER-AQ in the winter of 2013 near Fresno, and the Arvin O3 study in the summers of 2013/14 near Bakersfield), z_i budget terms, the surface pressure tendency, omega at the level nearest the observed ABL height (from the NARR data set), and subsidence. The surface pressure tendency and omega values are corrected to linear speeds via the hydrostatic approximation for the sake of comparison. Values in parentheses represent estimates of each term's 1 σ uncertainty.

	dO3/dt (ppb h^{-1})	O3 Advec (ppb h^{-1})	Dep O3 (ppb h^{-1})	Ent O3 (ppb h^{-1})	Δ O3 (ppb)	Photo Prod. (ppb h^{-1})	Avg O3 ABL (ppb)
1/16/13	0.70(0.002)	-0.02(0.01)	-0.91(0.59)	-0.75(0.32)	-5.0(1.0)	2.34(0.92)	38.4(1.5)
1/18/13	1.09(0.003)	-0.05(0.05)	-1.02(0.75)	-0.47(0.28)	-4.0(1.0)	2.63(1.08)	41.5(1.5)
1/20/13	0.72(0.002)	0.25(0.09)	-1.04(0.76)	-0.60(0.34)	-6.0(1.0)	2.10(1.18)	46.0(1.5)
1/21/13	1.15(0.003)	0.25(0.05)	-1.31(4.08)	0.08(0.37)	-8.0(1.0)	2.13(4.50)	52.2(1.5)
1/22/13	0.97(0.005)	-0.37(0.03)	-1.25(1.19)	-0.21(0.27)	-5.0(1.0)	2.87(1.50)	52.9(1.5)
1/30/13	2.21(0.001)	0.11(0.02)	-0.70(0.44)	-0.06(0.26)	-5.0(1.0)	3.39(0.72)	40.4(1.5)
2/4/13	2.19(0.003)	0.02(0.03)	-0.92(0.59)	-0.84(0.36)	-7.0(1.0)	3.92(0.98)	46.0(1.5)
Averages	1.29(0.003)	0.03(0.04)	-1.02(1.20)	-0.41(0.31)	-5.7(1.0)	2.77(1.56)	45.3(1.5)
Std Dev of Avg	0.64	0.21	0.21	0.35	1.38	0.68	5.68
6/26/13	2.48(0.002)	-2.19(0.16)	-0.82(0.75)	-6.55(0.73)	-40.0(1.0)	11.89(1.65)	60.0(1.5)
6/27/13	3.72(0.002)	-1.00(0.12)	-0.81(0.68)	-1.79(0.57)	-20.0(1.0)	7.33(1.37)	56.8(1.5)
6/28/13	3.12(0.002)	-1.54(0.13)	-1.02(0.60)	-1.20(0.66)	-16.0(1.0)	6.89(1.39)	72.9(1.5)
8/13/13	1.18(0.001)	-9.93(0.22)	-1.21(0.64)	-1.91(0.28)	-8.0(1.0)	14.23(1.14)	72.2(1.5)
8/14/13	2.35(0.002)	-2.48(0.23)	-1.28(0.71)	-0.96(0.40)	-10.0(1.0)	7.06(1.34)	79.2(1.5)
8/15/13	2.68(0.002)	-4.98(0.30)	-1.50(1.55)	-2.34(0.50)	-13.0(1.0)	11.51(2.35)	77.2(1.5)
9/28/13	3.71(0.001)	-0.66(0.06)	-1.31(0.82)	-2.29(0.24)	-10.0(1.0)	7.92(1.12)	61.3(1.5)
9/29/13	2.14(0.001)	0.23(0.03)	-1.65(1.57)	-1.77(0.26)	-6.0(1.0)	5.34(1.86)	66.2(1.5)
9/30/13	4.77(0.001)	-0.29(0.03)	-0.70(0.60)	-1.27(0.17)	-5.0(1.0)	7.04(0.80)	36.7(1.5)
6/8/14	2.73(0.002)	1.56(0.11)	-1.21(0.69)	-1.77(0.41)	-10.0(1.0)	4.15(1.21)	76.9(1.5)
6/9/14	1.65(0.002)	-0.34(0.07)	-1.49(0.81)	-2.77(0.51)	-10.0(1.0)	6.28(1.39)	92.2(1.5)
Averages	2.78(0.002)	-1.97(0.13)	-1.18(0.86)	-2.24(0.43)	-13.5(1.0)	8.15(1.42)	68.3(1.5)
Std Dev of Avg	1.02	2.14	0.31	1.53	9.79	3.07	14.63

Table 2: Ozone Budgets for the DISCOVER–AQ mission (top) and the ArvinO3 mission (below). Values in parentheses represent estimates of 1 σ uncertainties in each measurement.

	dCH4/dt (ppmv h^{-1})	CH4 advec (ppmv h^{-1})	CH4 Ent Flux (ppmv h^{-1})	Δ CH4 (ppmv)	CH4 Prod (Ggrams y^{-1})	Avg CH4 ABL (ppmv)
1/16/13	0.0231(0.006)	0.000(0.0004)	-0.056(0.046)	-0.40(0.05)	237.99(142.53)	2.13(0.002)
1/18/13	0.0260(0.0013)	0.004(0.0016)	-0.024(0.024)	-0.20(0.05)	131.43(80.45)	2.23(0.002)
1/20/13	-0.0029(0.0009)	0.008(0.0014)	-0.030(0.031)	-0.30(0.05)	58.37(103.47)	2.21(0.002)
1/21/13	-0.0100(0.009)	0.006(0.0043)	0.00(0.021)	-0.40(0.05)	-57.99(74.14)	2.31(0.002)
1/22/13	-0.1390(0.0018)	-0.01(0.01)	-0.019(0.024)	-0.30(0.05)	53.31(108.15)	2.29(0.002)
1/30/13	0.0254(0.0008)	-0.001(0.0013)	-0.022(0.021)	-0.20(0.05)	204.96(97.10)	2.02(0.002)
2/4/13	-0.0003(0.0005)	0.004(0.0021)	-0.024(0.021)	-0.20(0.05)	70.77(87.4)	2.07(0.002)
Averages	-0.011(0.001)	0.001(0.003)	-0.024(0.022)	-0.29(0.05)	99.83(99.03)	2.18(0.002)
Std Dev of Avg	0.06	0.01	0.02	0.09	100.64	0.11
6/26/13	0.0004(0.0001)	-0.006(0.0091)	-0.004(0.005)	-0.16(0.05)	254.80(96.26)	1.90(0.002)
6/27/13	-0.0014(0.0001)	-0.005(0.0047)	-0.007(0.008)	-0.15(0.05)	261.00(78.84)	1.87(0.002)
6/28/13	-0.0140(0.0004)	-0.013(0.0049)	-0.013(0.012)	-0.10(0.05)	282.00(116.24)	1.92(0.002)
8/13/13						
8/14/13						
8/15/13						
9/28/13	-0.0105(0.0004)	-0.005(0.0086)	-0.013(0.011)	-0.21(0.05)	117.00(88.78)	2.08(0.002)
9/29/13	-0.0019(0.0003)	0.01(0.0117)	-0.010(0.012)	-0.19(0.05)	16.00(90.65)	2.07(0.002)
9/30/13	-0.0066(0.0003)	0.005(0.0143)	-0.011(0.010)	-0.22(0.05)	-25.00(121.93)	1.94(0.002)
6/8/14	-0.0250(0.0006)	-0.011(0.0022)	-0.021(0.014)	-0.15(0.05)	150.50(96.52)	2.08(0.002)
6/9/14	-0.0150(0.0004)	-0.004(0.003)	-0.025(0.018)	-0.12(0.05)	300.00(114.88)	2.08(0.002)
Averages	-0.0092(0.0003)	-0.004(0.007)	0.013(0.011)	-0.16(0.05)	169.54(100.51)	1.99(0.002)
Std Dev of Avg	0.01	0.01	0.01	0.04	125.27	0.09

Table 3: Methane Budgets for the DISCOVER–AQ mission (top) and the ArvinO3 mission (below). Values in parentheses represent estimates of 1 σ uncertainties in each measurement.

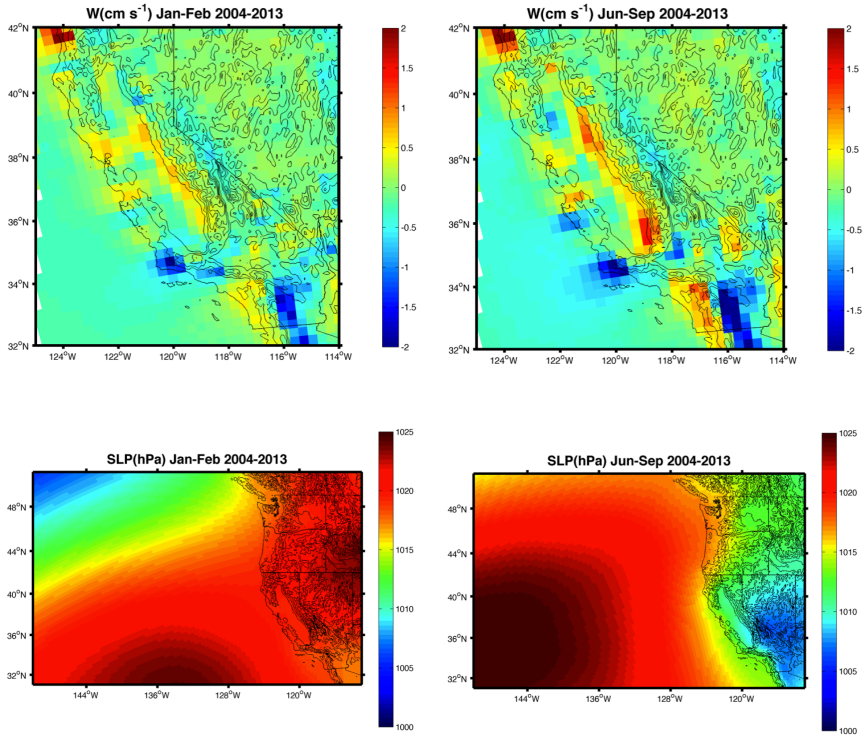

Figure 1: W (vertical velocity), converted from omega (pressure velocity), at the 900 hPa level and mean sea level surface pressure. Plotted for two intervals Jan–Feb and June–Sept. for 10 years from 2004–2013. The months chosen for the two separate plots represent the time frame of the flights.

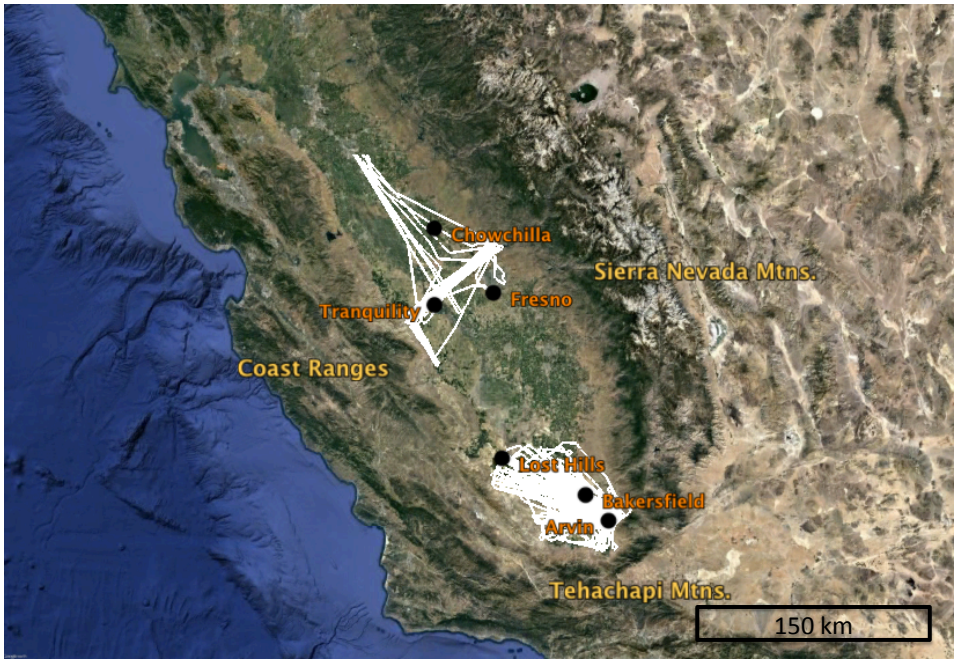

Figure 2: Flight paths of all data observed in the ABL for the two projects of this study: DISCOVER–AQ near Fresno from Jan/Feb 2013 (region 1), and the Arvin O3 project sampling from June–Sept over two summers and carefully mapping the inflow region upwind of Bakersfield and Arvin (region 2).

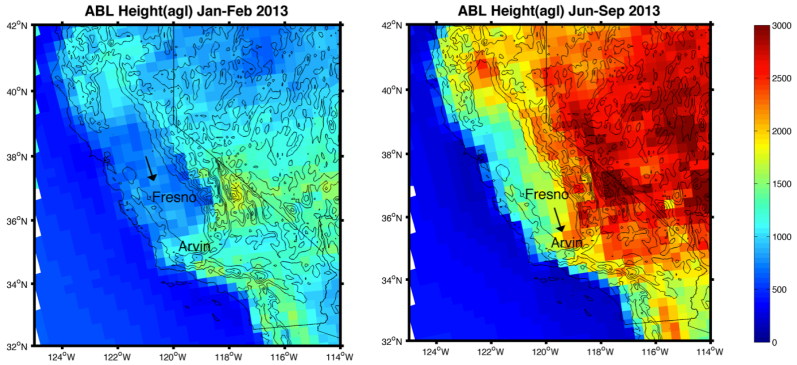

Figure 3: The average spatial pattern of boundary layer heights from the NCEP/NARR data set for (left) the winter period, and (right) the summer period of this study. Wind vectors represent the mean in situ winds measured by the aircraft near the ABL top.

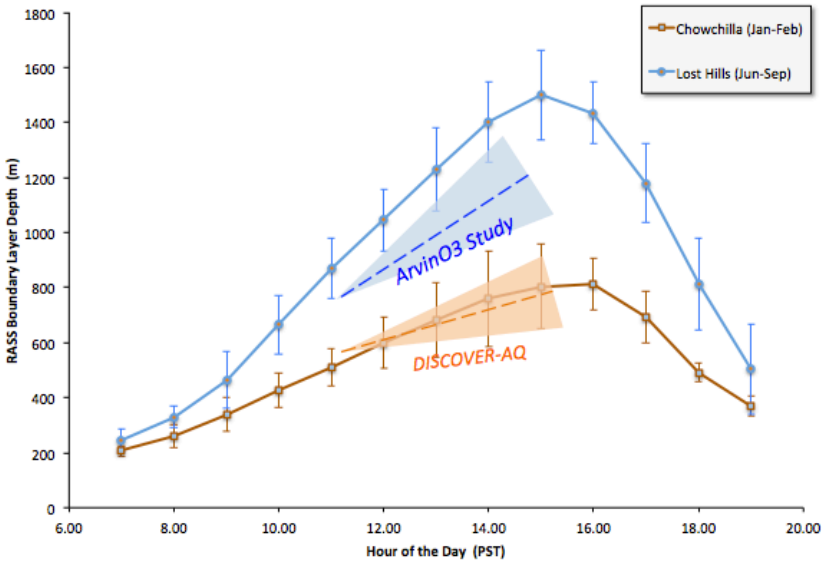

Figure 4: Diurnal boundary layer development as observed during the two experiments presented here, and the average data from the corresponding months and locations presented in Bianco et al. (2011).

5

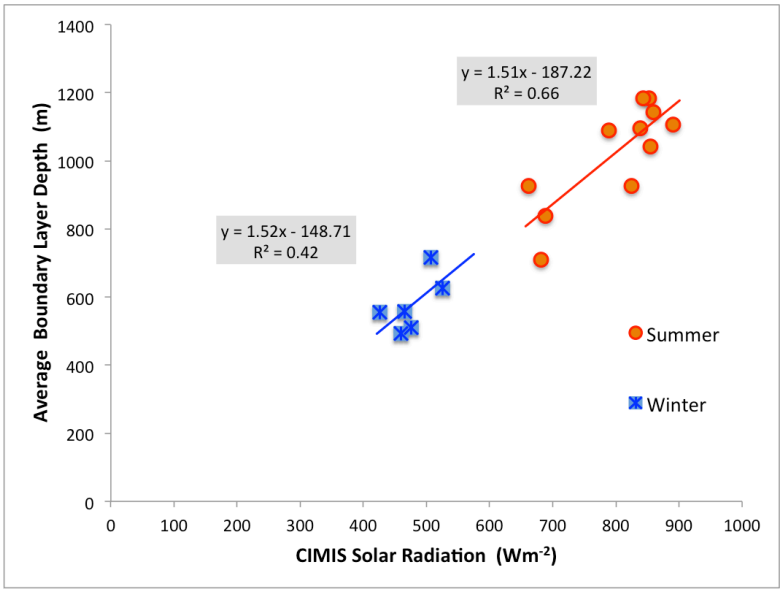

Figure 5: Flight averaged boundary layer depths as a function of the surface downwelling solar radiation as measured by the CIMIS station pyranometer in the flight regions near Fresno in winter, and Bakersfield in summer.

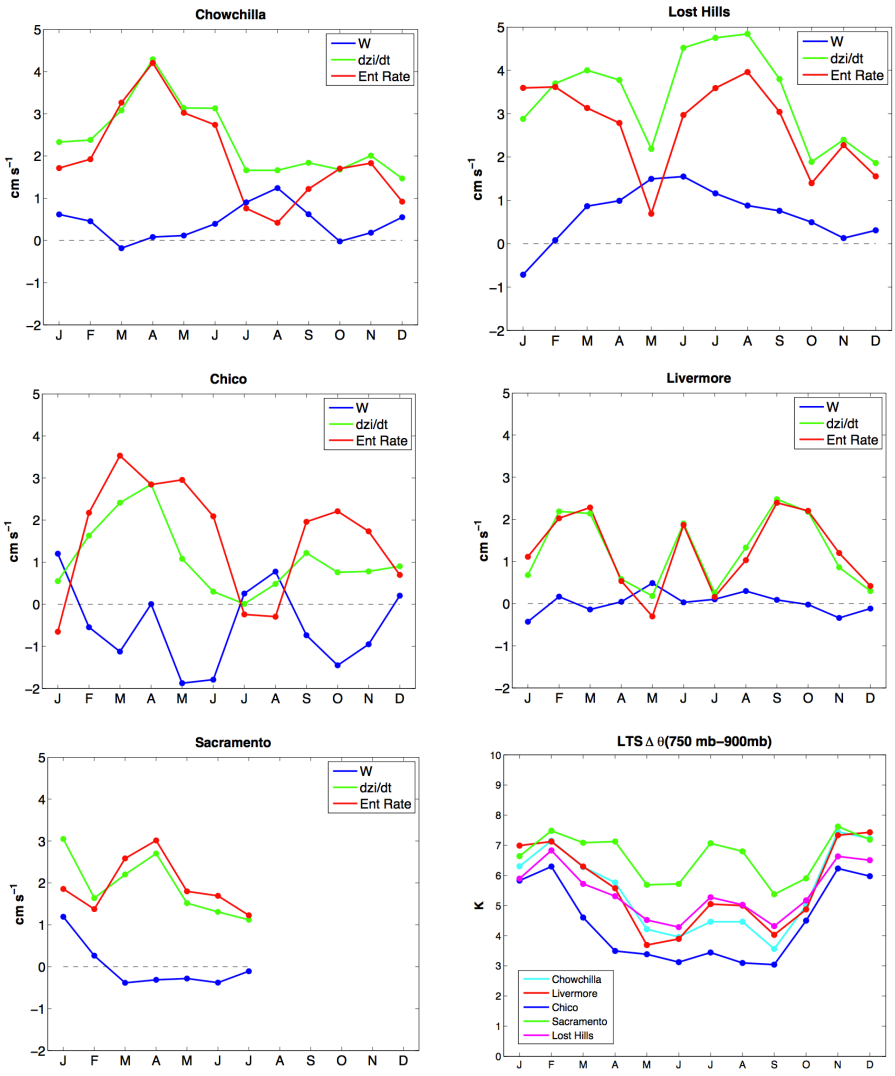

Figure 6: Observed monthly average ABL growth rates (dzi/dt, green lines) from the RASS network across the Central Valley described in Bianco et al. (2011) from the entire year of 2008. The mean vertical wind from the NCEP/NARR data set is included (blue lines) to yield estimates of entrainment (red lines). The lower right panel depicts the lower tropospheric stability (LTS) defined from the reanalysis data as the difference in potential temperatures at 750 and 900 hPa levels.

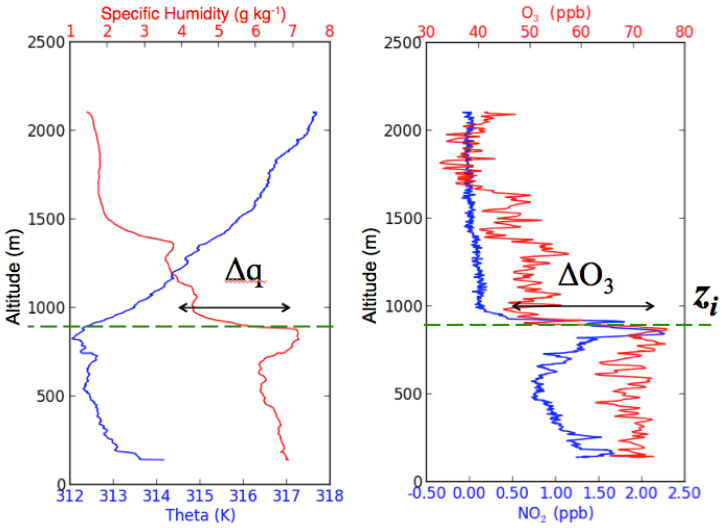

Figure 7: Example of vertical profiles of potentital temperature (theta) and specific humidity (q) on the left, and ozone and NO_2 observed on the right during the flight on 14 August 2013 near Bakersfield, CA. Z_i is the estimated height of the ABL determined by the scalar jump (Δq and ΔO_3 shown here) across the entrainment zone.

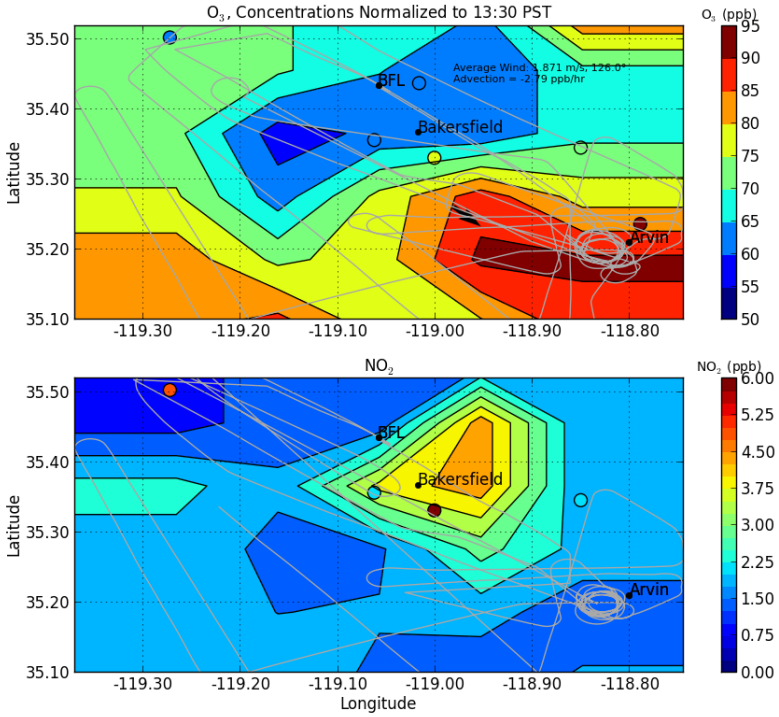

Figure 8: Horizontal patterns of O_3 (top) and NO_2 (bottom) during an ozone exceedance episode near Bakersfield on 14 August 2013. The grey lines represent the flight tracks, and the coloured circles represent the surface network observations. Because of the continual trend in ozone throughout the flight, the values in the top figure are all corrected to a reference time of 13:30 PST. The black arrow in the top figure represents the vector average wind observed in the ABL during that sortie showing a strong negative advection of ozone and a large positive advection of NO_2 into the Arvin region to the south. BFL is the Meadows Field Airport on the north end of urban Bakersfield. The coloured circles represent the 13:00-14:00 surface site measurements from the ARB surface network.

Ian Faloona 9/13/2016 9:44 PM
Deleted: a

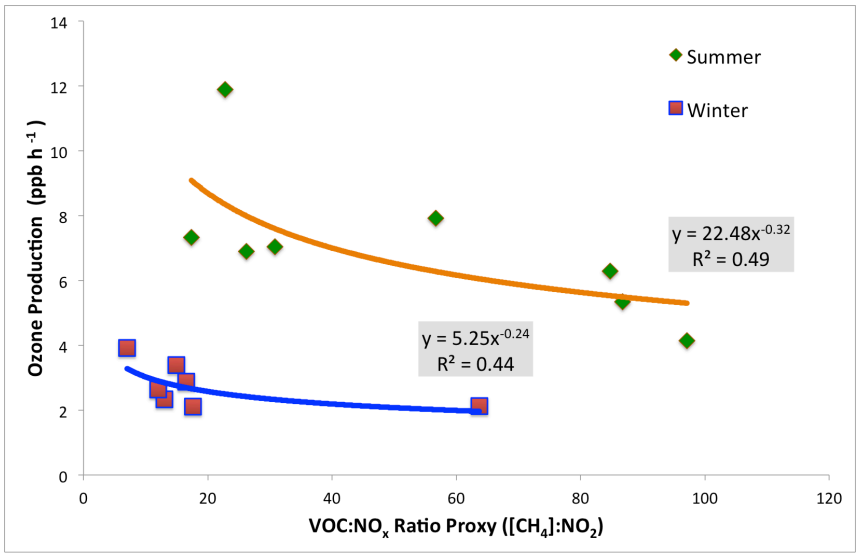

Figure 9: Plot of measured ozone production from the DISCOVER-AQ campaign near Fresno during winter (maroon squares) and from the ArvinO3 study during the summer (green diamonds) versus a proxy of VOC:NO_x ratio estimated by the measured CH_4 enhancement over global background divided by the NO_x measured during the flights from the CARB air quality monitoring network nearby.

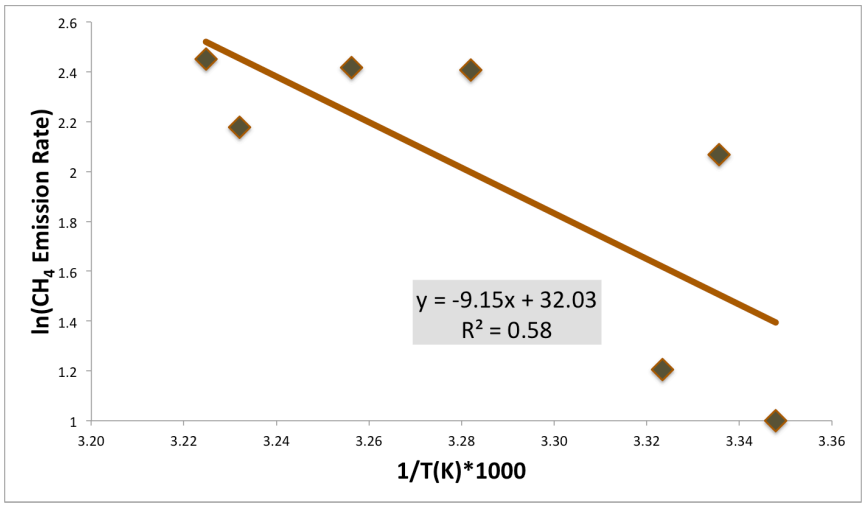

Figure 10: Arrhenius plot of the estimated methane emission rate from each flight and the average ABL temperature from the ArvinO3 study where methane emissions are believed to be dominated by agricultural sources.

5